thesis for the degree of licentiate in Applied acoustics

A ground-borne noise prediction model for railway traffic in tunnels in bedrock

Fatemeh Dashti

Department of Architecture and Civil Engineering
Division of Applied Acoustics
Chalmers University of Technology
Gothenburg, Sweden, 2023

A ground-borne noise prediction model for railway traffic in tunnels in bedrock

Fatemeh Dashti

Thesis for the degree of Licentiate
Series name: Lic / Architecture and Civil Engineering / Chalmers University of Technology

Department of Architecture and Civil Engineering
Division of Applied Acoustics
Chalmers University of Technology
SE-412 96 Gothenburg, Sweden
Phone: +46 (0)31 772 1000
www.chalmers.se

Printed by Chalmers Reproservice
Gothenburg, Sweden, 2023

Abstract

Human life has become more manageable by the expansion of railway lines. However, despite providing convenience, railways increase noise and vibration in residential areas. Vibrations and noise generated by railways may harm human health, cause cosmetic damage and have an adverse impact on the environment. In order to reduce the effects of train-induced noise and vibration, efficient and accurate models for the prediction of ground-borne noise and vibration are required.

Various analytical, theoretical, and experimental models have been developed to predict ground-borne noise. There is generally a lack of published information about parameters for ground-borne noise prediction concerning Swedish conditions with bedrock of high quality. Some investigations are reported, and a few consultancy companies have their own developed models, which are generally not publicly available. In fact, overall, the input data used to form these models and the methods of validation are not publicly available. Moreover, the statistical nature of the source and transfer paths requires that uncertainties are accurately handled in the model.

This work aims to develop a model for ground-borne noise prediction for underground tunnels, to be used in Swedish Transport Administration projects. The methodology is formulated for three different stages based on precision and available information: location stage, planning stage, and construction stage. The first two stages correspond to planning and designing a railway track. The third stage involves the construction stage where more detailed information may be acquired. The prediction model presented here is developed for Swedish bedrock up to 1 kHz and formulated as a source term and several correction terms. These terms take into account various aspects, including train speed, distance attenuation, ground-to-building coupling, vibration levels on different floors and walls, how the room properties affect sound pressure levels within rooms, and different track treatments. Moreover, uncertainties are estimated using the standard deviation of each term. The required data are gathered from measurements in the Gårda tunnel in Gothenburg combined with existing data from measurements in the Åsa tunnel close to Varberg.

As a result, a comprehensive model is suggested for ground-borne noise prediction in Swedish Transport Administration projects. However, the model is still under development, will be sent upon referral, and may undergo improvements.

Keywords: Ground-borne noise and vibration, Railway tunnel induced vibration, Wave propagation in bedrock, Prediction of noise.

Preface

This licentiate thesis has been carried out in the Division of Applied Acoustics, Department of Architecture and Civil Engineering at Chalmers University of Technology. The project was financed by the Swedish Transport Administration.

First I would like to thank my supervisor Patrik Höstmad and Co-Supervisor Jens Forssén whose expertise and continuous encouragement have shaped the direction of this study. Their valuable insights, constructive feedback, and unending dedication have inspired me to reach new heights.

Wolfgang, as the head of Applied Acoustics, I am deeply thankful for your invaluable advice and support.

I would like to thank my friends and colleagues at the Applied Acoustics Division for all their contributions by offering support and amusement. Thank you Jens A., Astrid, Monica, Börje, Jannik, Hannes, Tommi, Leon, Elin.

I would like to thank Trafikverket individuals, Maria Luisa Botella, Alf Ekblad, Magnus Källman, and Peter Lindquist for their constructive collaboration and comments. They have generously provided us with valuable information and measurement data. Your willingness to share these resources has significantly enhanced our study's quality and comprehensiveness.

I also thank Johan Scheuer for his valuable contributions to measurements, data, and knowledge.

I would like to express my gratitude to the reference group of engineers and researchers assigned to the project for their constructive comments and thoughtful suggestions and their willingness to share models, reports, and know-how.

Finally, I am thankful to my close friends Ehsan G. and Nata and of course my family for all their support.

Gothenburg, October 2023
Fatemeh Dashti

Thesis

This thesis consists of an extended summary and the following appendixes.

[**Paper**] **F. Dashti, P. Höstmad, J. Forssén**. Finite element modelling of tunnel shielding in vibration measurements of ground-borne noise. *14th International Workshop On Railway Noise (IWRN14)*, China, Shanghai (2022).

[**Report**] **F. Dashti, J. Forssén, P. Höstmad**. Ground Borne Noise Model and Methodology Description. Tech. Rep. Division of Applied Acoustics, Department of Architecture and Civil Engineering, Chalmers University of Technology, Gothenburg (2023).

Contents

Part I

Overview

CHAPTER 1

Introduction

1.1 Background

The focus of this study is the development of a model and methodology for ground-borne noise. However, a wider background is presented here.

Noise and vibration are interconnected phenomena affecting human well-being and the environment significantly. Noise refers to unwanted sounds that can disrupt communication, cause annoyance, and even lead to health issues, while vibration refers to mechanical oscillations or movements. Industrial activities, transportation systems, construction sites, or even natural events such as earthquakes cause vibration and noise. Railway systems, as a source of generating noise and vibration, significantly impact nearby communities and the environment. Rail noise is mainly caused by train wheels rolling on the tracks, aerodynamic noise, and other mechanical noise [1], whereas train movements and energy transfer between the rails and the ground primarily cause vibrations.

Sustainable and healthier living requires a better understanding of the railway sources and surrounding areas, predicting noise and vibration levels from railway sources, and reducing generated noise and vibration levels. To do so, it is necessary first to collect relevant data, including train characteristics, track conditions, topography, and particularities of the surrounding environment. The second step is to develop prediction models to estimate noise and vibration levels along a railroad line at specific locations. Finally, appropriate mitigation measures can be planned and implemented based on the predic-

tion model to reduce noise and vibration levels. This study focuses on the second step and only noise estimation, i.e., developing a prediction model for ground-borne noise.

This ground-borne noise prediction model focuses on assessing and predicting noise generated by transportation systems, particularly railways, and their impact on the environment and structures. Reliable prediction of ground-borne noise is vital when choosing the location of the track. It is also crucial before constructing a new railway in tunnels or on the ground surface close to residential areas and vice versa.

Various models have been developed by groups or individuals to predict ground-borne noise: some of them are described in section 1.5.2. However, there is still a need to obtain more knowledge in order to analyze ground-borne noise caused by railway traffic in tunnels and develop prediction models with high precision. There are generally no published parameters for predicting ground-borne noise concerning Swedish bedrock conditions. Bedrock in Sweden is often of high quality and may have few cracks, so the frequency range of interest for ground-borne noise generated by railways in Swedish bedrock can approach 1000 Hz, however based on the results in this work, upper frequency for ground-borne noise approach to around 500 Hz. According to Trafikverket standards the limit maximum level value for ground-borne noise indoor is 32 dBA (time-weighting Fast) [2]. These standards are particularly applicable to new infrastructure and nighttime conditions.

Furthermore, in the context of ground-borne noise prediction, there are several sources of statistical variation and uncertainties that influence the accuracy of the models. These uncertainties arise due to various factors, including variations in source characteristics, ground properties, wave propagation, building characteristics and interaction, and other environmental factors. Given these common uncertainties, the methodology and model need to handle the data using a statistical approach to account for variability and provide more robust predictions. Although empirical models have been developed to predict ground-borne noise, few studies address the statistical approach for dealing with uncertainty in these empirical predictions [3]. In this study, statistical approaches are used to handle the uncertainties of each term and estimate the final uncertainty of the sound pressure level in the room.

1.2 Objectives

The specific purpose of the present project is to develop a methodology and model for prediction of ground-borne noise generated by trains passing through a tunnel in projects managed by the Swedish Transport Administration. The model is developed based on numerical and empirical data types and from sev-

eral data sources, including measurements carried out in some railway tunnels in Sweden. The selection of the model and its parameters is determined so that essential aspects are considered up to 1000 Hz. Since the available measurement data predominantly pertain to tunnels in dense bedrock, the presented model is most suitable for similar geotechnical conditions. Additionally, the standard deviation of each term is calculated to address final uncertainties in source terms, propagation terms, and receiver terms.

The methodology of the noise prediction model is categorized into three stages based on their accuracy and available information: location stage, planning stage, and construction stage. The location stage is utilized at the early stages of project development where few input parameters are available, such as railway system type, train characteristics, geotechnical conditions, and building sensitivity. Typical and simplified values can then be used for the terms. The model employs single numbers at this stage. The planning stage is employed at the design stage where more input data are available. These models provide more accurate quantification of vibration severity and precise location identification along the railway compared to early-stage models. The precision of the result will be higher at the location stage and parameters formulated in 1/3-octave bands are used. The construction stage is employed during the construction of a railway track or tunnel. This stage is used to enhance the accuracy of model parameters or to validate and adjust predictions made during the planning stage based on site-specific measurements. For instance, when constructing a tunnel, vibration levels in the building can be monitored while drilling and blasting in the tunnel. The purpose of such monitoring is to ensure that vibration limits are not exceeded during construction. Data from these on-site measurements are valuable for refining the prediction.

In addition, an outcome of the project is to raise the level of knowledge in design methodology for ground-borne noise through continuous communication and the dissemination of results to industry, society, and academia.

1.3 Limitations

The model delivered here focuses on situations with railway tunnels and building foundations in bedrock. In order to validate the suggested model, additional measurements are needed. Valuable information can be gained to determine significant properties during the construction stage by evaluating various vibration sources like hydraulic hammers and their corresponding measurement methods. More comprehensive numerical simulations are necessary to enhance the understanding of dispersion within building structures and through rocks with special properties. Furthermore, no special cases with

complex bedrock geometry or largely influential crack zones are considered.

There are generally significant uncertainties in the propagation of vibrations from tunnels through the rock to buildings in cases where there are fracture zones or the rock geometry is special. There is also uncertainty regarding the ground-to-building connection and vibration propagation within a building. Further development of the model requires more consideration of these areas of potential influence.

1.4 Fundamentals of ground-borne noise

1.4.1 Wave types in ground-borne noise

Wave motion in a solid medium can be categorized into two types: body waves and surface waves. A body wave travels through the ground, while a surface wave travels at the ground's surface. There are two types of body waves: pressure waves (P-waves) and shear waves (S-waves). P-waves are the quickest seismic waves that travel parallel to particle motion. S-waves propagate perpendicular to particle motion, as the second fastest type of seismic wave. As the vibrations reach the ground surface, they continue to propagate as surface waves, and reflections also occur. There are two primary types of surface waves: Rayleigh waves and Love waves. A Rayleigh wave causes the surface to rotate in the opposite direction of the wave propagation. Love waves appear only if the top soil layer is softer than the lower soil layers. Love waves are not common. Figure 1.1 shows how different wave types propagate in the ground.

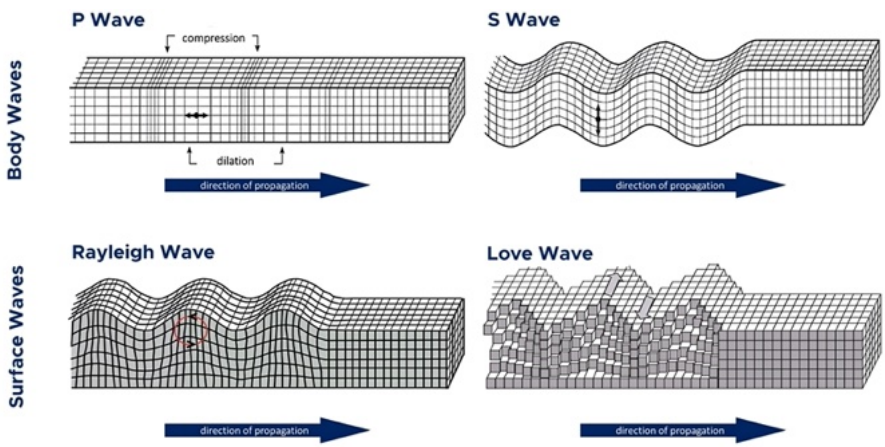

Figure 1.1: Seismic wave type. Adapted from Wikipedia [4].

Different waves propagate at different speeds in a medium. Eq 1.1 and 1.2

show speeds of P-wave (C_{P}) and S-wave (C_{S}), respectively.

$$C_{\mathrm{P}} = \sqrt{\frac{E(1-\nu)}{\rho(1-2\nu)(1+\nu)}} \tag{1.1}$$

$$C_{\mathrm{S}} = \sqrt{\frac{G}{\rho}} \tag{1.2}$$

where E is Young's modulus, ν is Poisson's ratio, ρ is density of the soil and G is shear modulus.

R-waves can be generated by the interaction of two body waves at the ground surface. The following expression can be used to estimate the speed of the R-wave, C_{R} [5].

$$C_{\mathrm{R}} \approx \frac{0.87 + 1.12\nu}{1+\nu} C_{\mathrm{S}} \tag{1.3}$$

1.4.2 Wave propagation

The amplitude of vibrations radiated from a source attenuates by increasing distance from the source, where vibration energy decreases due to geometrical damping and material damping. Geometrical damping is caused by increasing the geometrical spread of the energy at the wavefront. The attenuation induced by geometrical damping is frequency-independent but depends on the source and wave type. In material damping, energy is lost during each cycle of deformation. Geometrical damping has a relatively weaker impact on Rayleigh waves compared to its effect on body waves. However, Rayleigh waves can still lose energy due to the material damping. Since Rayleigh waves have a lower attenuation, they carry most vibration energy at a distance from the source. The attenuation due to geometrical and material damping can be modeled, using Lamb's equation, as

$$v = v_1 \left(\frac{r_1}{r}\right)^m e^{-\alpha(r-r_1)} \tag{1.4}$$

where v_1 is vibration amplitude at distance r_1 from the source, v is vibration amplitude at distance r from the source, the exponent m is a constant that determines geometrical attenuation power based on wave type and source type, and α is the damping coefficient for the material damping. The damping coefficient describes the rate of damping and energy loss, where a higher damping coefficient results in faster energy dissipation. The damping coefficient is affected by some factors such as material property and excitation frequency. Table 1.1 shows an example of the damping coefficient range for a frequency of 50 Hz.

Table 1.2 shows the exponent m for geometrical damping based on various wave types and sources of vibration. When a building is far enough from the rail, a train can be modeled as a moving point source. Additionally, a train behaves like a point source when it passes through switches or navigates curves. At shorter distances between the rail and the building, a train can be modeled as a line source. Ground-borne noise is generally pronounced at closer distances from the railway and when a train passes through a tunnel it can be considered as a line source. The vibrations generated by tunnel railways are predominantly caused by P-waves [6]. It means the geometrical damping causes the vibration amplitude to decrease by 3 dB per distance doubling.

Table 1.1: Values of damping coefficient for 50 Hz [7].

Soil class	Damping coefficient α (1/m)
Soft soils like loose clay	0.1–0.3
Firm soils like solid clay	0.03–0.1
Stiff soils like very stiff clay	0.003–0.03
Stiff bedrock	<0.003

Table 1.2: Values of the constant m [8], [9].

Wave type	Point source	Line source
P-wave	1	0.5
S-wave	1	0.5
R-wave	0.5	0

1.4.3 Reflection and refraction

The propagation of seismic waves in the ground is governed by complex interactions involving reflections and refractions. When seismic waves encounter boundaries between geological layers or structures, they exhibit distinct behavior. Some waves return back towards the source (reflection) and some continue to travel through the new material (refraction). The amplitudes and angles of both reflected and refracted waves are influenced by factors such as wave speed and material properties.

1.4.4 Wave coupling phenomena and challenges in underground tunnels

The behavior of waves within a tunnel is a complex phenomenon that varies with the frequency of the waves. At low frequencies, the entire tunnel structure experiences noticeable up-and-down movement. As frequencies increase, the involvement of shear waves results in different modes of oscillation and deformation within the tunnel.

The underground tunnel railway generates P-waves that travel through the surrounding environment. As these P-waves encounter different layers or interfaces between rock types, they can partially convert into S-waves due to changes in the materials' behavior. Furthermore, seismic waves interact with the ground's surface, and they can cause surface waves, such as Rayleigh and Love waves. These surface waves can be generated from the conversion of P and S-waves as they interact with the free surface of the ground. This transformation and wave coupling, combined with the uncertainties in the medium, create complexities that challenge the use of deterministic models. Considering these difficulties, statistical models and experimental approaches become increasingly relevant. Statistical models can account for uncertainties and provide a more probabilistic view of wave propagation from a tunnel.

1.4.5 Wave propagation in rocks

Different types of rock exhibit different wave propagation characteristics. A bedrock's effect on wave propagation is determined by its scale. Small samples of rocks are typically considered intact [10]. The wave propagation in intact rocks depends on physical properties such as texture, density, porosity, stresses, and water content. Wave propagation in large-scale rocks like tunnel constructions is mainly influenced by discontinuities and boundaries between geological regions. In addition to material losses, discontinuities and impedance differences between geological regions cause wave attenuation in rock masses. Reflections and refractions cause coupling waves in discontinuities. Frequency is another important parameter of propagating waves. If the frequency is high, then most of the wave is reflected, while if the frequency is low, then most of the wave is transmitted across the discontinuity [11].

1.4.6 Ground-borne noise and vibration

Vibrations transmitted through the ground are known as ground-borne vibrations. In this case, vibrations are propagated through the ground by sources, such as railway trains, and may reach the foundation of a building. Vibration passes through the structure of the building and can be perceived as whole-

body vibration. A common frequency range for ground-borne vibration is between 1 to 80 Hz [12].

Ground-borne noise experiences the same process as ground-borne vibration. When vibration waves reach a building, they can cause vibrations in the building's foundation, walls, floors, and other components. Vibrating structure results in sound waves that can be perceived as audible noise. Ground-borne noise is common when a railway tunnel and a building are situated on the same bedrock. The common frequency range for ground-borne noise is 20–250 Hz [12]. For bedrock in Sweden, the frequency range of interest may approach 1000 Hz. However, as distance increases, higher frequencies experience more attenuation. Therefore, at further distances from the source, the upper limit of the frequency range of interest becomes lower than 1000 Hz.

1.4.7 Vibration and noise in buildings due to underground railways

Trains moving on underground railways excite the rails and the underlying track structure. As a result, these vibrations propagate into the surrounding ground, i.e., rock and soil. Several factors affect the vibration generated by a train when the vibration propagates from a tunnel to a building. The vibration paths can be divided into three stages: source, path of propagation, and receiver. The propagating path of the vibration is illustrated in Figure 1.2. The prediction and mitigation of vibration problems require an understanding of how each of these three steps affects the vibration situation. In the following, each path is described.

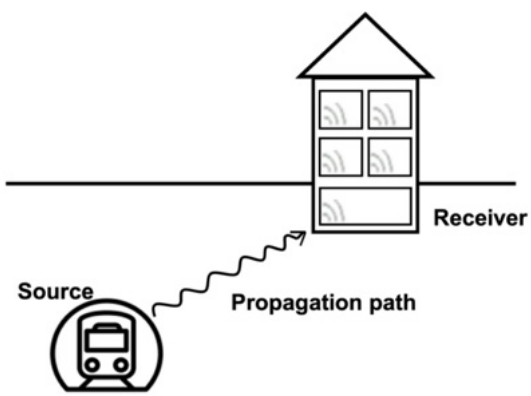

Figure 1.2: Propagation path.

Source of vibration

The source of vibration is the movement of the train along the track and the interaction between the wheel, rail, and track structure. Parameters that affect the level of vibration induced by trains passing through the tunnel are, for instance, train speed, axle load, car body suspension, unsprung mass, and wheel and rail conditions [13], [14].

The increased speed of the train will generally cause a higher vibration level in the tunnel. According to Kurzweil [15], doubling a train's speed will result in a 4 to 6 dB increase in vibration levels. Vibrations are largely influenced by the composition of trains, e.g., the largest vibrations are observed when all wagons carry uniform cargo, such as timber, oil and ore [13]. The axle load will also increase the dynamic loading generated by the train. By doubling the axle load, the tunnel vibration levels will increase by 2 to 4 dB [15]. The level of ground vibration can be reduced by 6 dB by halving the unsprung mass [16]. Moreover, resilient wheels can significantly reduce ground vibration above 20 Hz compared with standard wheels [17].

Propagation of vibration to building

Vibrations propagate through the rail and sleeper to the substructure, which is usually ballast made from crushed rocks. Ballast is usually located directly on the rock in regular Swedish tunnels [18]. Ballast mats can be used in the ballast if an increased amount of damping is required. Floating slabs are employed for tunnels in various contexts, including those near hospitals, museums, or concert halls, where high attenuation is necessary [18].

Vibrations propagate as surface waves through the walls and roof of the tunnel and then spread away from the tunnel. Vibration levels generated from tunnels built on bedrock are generally lower than those of tunnels in soil. According to Ungar and Bender [6], at lower frequencies, tunnel vibration levels in soil are about 5 dB higher than those in bedrock, and at higher frequencies, they are about 12 dB higher.

The vibration propagates through the substructure around the tunnel in the form of body waves, i.e., S-waves and P-waves. When considering the vibrations of the ground, S-waves can be neglected because of their greater attenuation than P-waves [6]. The vibrations attenuate during propagation due to geometrical and material damping. In rock, the vibration attenuation is small and primarily caused by the geometric spreading of the vibration energy [6], [15].

Receiver

When the vibrations propagate through the ground, they eventually reach the receiver, the foundation of nearby buildings. The coupling between the ground and the foundation affects the amount of vibration transmitted to the building. According to FTA model [19], coupling loss for the foundation in the soil is -5 dB for wood-frame houses; -7 dB for 1-2 story masonry; -10 dB for 3-4 story masonry; -10 dB for large masonry on piles; and -13 dB for large masonry on spread footings. While for a building supported directly on the rock, the coupling loss is small (often assumed to be neglectable).

The vibrations propagate from the foundation into other parts of the building, making floors, walls, and ceilings vibrate as well. In a building, walls and ceilings generally resonate between 10 and 60 Hz. The whole building's resonance may occur below 10 Hz [20].

Depending on the frequency, vibrations may be felt as whole-body vibrations (ground-borne vibration) or be heard as low-frequency rumbles, i.e., structurally radiated noise (ground-borne noise). According to Kurzweil [15], in heavy buildings, vibration levels decrease as height increases from 1 to 3-4 dB per floor, whereas in lightweight buildings, vibration levels do not change with height. Vibrations on the upper floors of lightweight buildings can sometimes be amplified by floor resonances.

When vibration travels through the building, the vibrations of the walls, floors, and ceilings will emit noise. The generated noise level in a room will differ according to the size and shape of the room, the amount of sound absorption, and surfaces' vibration [21]. Based on Melke's suggestion [22], the sound pressure level in a room can be estimated by the following formula:

$$L_{\mathrm{p}} = L_{\mathrm{v}} + 10\log_{10}\sigma + 10\log_{10}\left(\frac{4S}{A}\right) \qquad \text{(dB)} \tag{1.5}$$

where L_{p} is the sound pressure level (dB re 20 μPa), L_{v} is the vibration velocity level (dB re 50 nm/s), σ is the radiation efficiency(-), S is the area of the vibrating surface (m^2), and A is the absorption area of the room (m^2 Sabine). A simplified formula presented in the European project RIVAS [23] can be used for prediction at the engineering level under certain assumptions of room size 10 m^2 and the reverberation time of 0.5 s as

$$L_{\mathrm{p,av}} \approx L_{\mathrm{v,meas\text{-}floor}} + 7 \qquad \text{(dB)} \tag{1.6}$$

where $L_{\mathrm{v,meas\text{-}floor}}$ is floor velocity level measured at mid-span (dB re 50 nm/s) and $L_{\mathrm{p,av}}$ is space average sound levels (dB re 20 μPa). Michel et al. [24] suggested a further simplified model by assuming that the space average sound level is 3 dB higher than the sound level measured in the room center as

$$L_{\mathrm{p,mes}} \approx L_{\mathrm{v,meas\text{-}floor}} + 4 \qquad \text{(dB)} \tag{1.7}$$

where $L_{\mathrm{p,mes}}$ is the sound pressure level measured in the room center (dB re 20 μPa).

1.5 State of the art of existing models

1.5.1 Existing models

Ground-borne noise and vibrations induced by railways negatively impact urban areas. It is crucial to accurately measure and predict noise levels in order to protect the health and well-being of the public. Different models have been developed to measure existing noise sources, predict the impact of upcoming sources, and compare noise levels in different areas.

Common models for the prediction of ground-borne noise and vibrations include empirical [15], [25], analytical [26], and finite element models (FEM) [27], [28], as well as hybrid models [29], [30]. An empirical model uses measurements to provide a quick estimation of noise and vibration levels on the ground, whereas an analytical model predicts noise and vibration using mathematical and physics-based calculations, allowing for a deeper understanding of the underlying physics. In FEM models, structural dynamics and soil-structure interactions are considered as well as the vibrational response of complex structures. A hybrid model combines different approaches to provide more accurate predictions. Model selection depends on factors such as problem complexity, data availability, computational resources, and accuracy requirements.

Ground-borne noise prediction models generally follow a similar structure with a source term followed by correction terms that take into account a variety of phenomena and cases. There are a number of factors to consider, including train speed, distance attenuation, coupling ground to building, and how vibration levels on walls and floors affect sound pressure levels. It is usually assumed that terms and factors are independent, so they can be treated independently.

Some well-known models are presented in the following.

Model suggested by Kurzweil

Kurzweil [15] presents a method for estimating A-weighted sound pressure levels as well as noise and vibration spectra due to train-generated ground-borne vibration in buildings, in octave bands.

The floor vibration level, $L_{\mathrm{a(room)}}$ (dB re 10^{-6} g(rms)), in a building near

a subway, is estimated as

$$L_{\mathrm{a(room)}} = L_{\mathrm{a(tunnel\ wall)}} - C_{\mathrm{g}} - C_{\mathrm{gb}} - C_{\mathrm{b}} \qquad \text{(dB)} \tag{1.8}$$

where

$L_{\mathrm{a(tunnel\ wall)}}$ is the octave band acceleration of the wall of a subway tunnel during a train pass-by (dB re 10^{-6} g(rms))

C_{g} is the vibration attenuation due to propagation through the ground (dB)

C_{gb} is the vibration attenuation (coupling loss) between the ground and the building (dB)

C_{b} is the vibration attenuation due to the propagation in the building (dB).

These corrections are adapted from references such as [31] and [32].

Tunnel wall vibration level, L_{a}

A range of measurements for both ballasted and direct fixation rail fastening systems (not floating slab track) were made in earth-based concrete tunnel structures.

Vibration attenuation in soil ground, C_{g}(soil)

To calculate the vibration spectrum in soil at a given distance from the tunnel wall, the correction shown in Figure 1.3 is subtracted from the octave-band levels selected from the tunnel wall vibration spectra at the desired distance. Figure 1.3 illustrates the attenuation in ground vibration levels, C_g (soil), resulting from propagation in soil. The graph displays this attenuation for various distances from the wall of an earth-based tunnel across different frequencies.

Vibration attenuation in rock, C_{g}(rock)

In rock, the geometric attenuation is defined as Eq. 1.9, for distances up to about half the train length.

$$C_{\mathrm{g(rock)}} = 10 \log_{10} \left(\frac{R_0 + X}{R_0} \right) \qquad \text{(dB)} \tag{1.9}$$

where R_0 is the distance from the tunnel center to the tunnel's outer wall surface (m) and X is the distance from that surface to an observation point (m).

Coupling loss between ground and building, C_{gb}

- For lightweight frame buildings and slab foundations on grade the coupling loss, C_{gb}, is 0 dB
- For buildings with footings very close to the tunnel structure, a coupling loss of 10 to 20 dB can be introduced using resilient material between the building and the structure

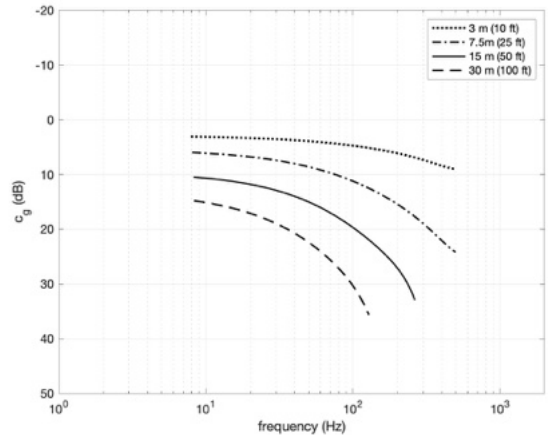

Figure 1.3: Vibration attenuation due to propagation through the ground. Adapted from reference [15].

- Otherwise the coupling loss is 0 dB.

Vibration attenuation in a building, C_b
The vibration levels typically decrease by 3 dB per floor, starting at the ground level, whereas for lightweight constructions no decrease with height is found.

Resulting structure-borne noise in buildings
An estimation of the relationship between the room floor acceleration level, $L_{a(room)}$, and the resulting sound pressure level in the room, $L_{p(room)}$ (dB re 20 μPa), is provided in Eq. 1.10 :

$$L_{p(room)} = L_{a(room)} - 20 \log_{10} f + 37 \text{ (dB)} \tag{1.10}$$

where f is the octave-band center frequency (Hz).

BanaMarkPRO model

The model BanaMarkPRO is a development at Region Stockholm (SLL), based on the Danish model "Vibration from Railway traffic" (Banestyrelsen, 2000). It predicts ground-borne vibration in soil in 1/3-octave bands for a frequency range of 2.5 to 200 Hz.

The model for the prediction of ground-borne vibration transmitting from the track to the receiver is presented in the following, in which Eq. 1.11 and 1.12 calculate vibration level at the first and top floor, respectively.

$$L = L_{\mathrm{Ref}} - \Delta L_{\mathrm{m}} - \Delta L_{\mathrm{e}} - \Delta L_{\mathrm{v,geo}} - \Delta L_{\mathrm{v,tab}} - \Delta L_{\mathrm{b}} - \Delta L_{\mathrm{fl}} \tag{1.11}$$

$$L = L_{\mathrm{Ref}} - \Delta L_{\mathrm{m}} - \Delta L_{\mathrm{e}} - \Delta L_{\mathrm{v,geo}} - \Delta L_{\mathrm{v,tab}} - \Delta L_{\mathrm{b}} - \Delta L_{\mathrm{ff}} \tag{1.12}$$

where

L_{Ref} is the reference vibration level (dB re 50 nm/s), measured at $R_{\mathrm{ref}} = 8$ m from the track center

ΔL_{m} is attenuation in the ballast (dB)

ΔL_{e} is vibration attenuation from the track located at embankments or cuttings (dB)

$\Delta L_{\mathrm{v,geo}}$ is geometrical attenuation (dB)

$\Delta L_{\mathrm{v,tab}}$ is frequency dependent hysteretic attenuation (dB)

ΔL_{b} is vibration transfer from soil to foundation building (dB)

ΔL_{fl} is vibration transfer from foundation to ground floor (dB)

ΔL_{ff} is vibration transfer from foundation to top floor (dB).
$\Delta L_{\mathrm{v,geo}}$ and $\Delta L_{\mathrm{v,tab}}$ are calculated by Eq. 1.13 and 1.14, respectively, and other parameters are obtained from the report (Banestyrelsen 2000):

$$\Delta L_{\mathrm{v,geo}} = -11 \log_{10}(R/R_{\mathrm{ref}}) \qquad (\mathrm{dB}) \tag{1.13}$$

$$\Delta L_{\mathrm{v,tab}} = 10 \log_{10}(e^{-2\pi f \eta (R - R_{\mathrm{ref}})/c}) \qquad (\mathrm{dB}) \tag{1.14}$$

where $\eta = 0.03$ and the Rayleigh wave speed c is 200 m/s.

The diffuse field sound pressure level caused by the vibrations is expressed as follows.

$$L_{\mathrm{p}} = L_{\mathrm{v(ref\ 50\ nm/s)}} + 10 \log_{10}(S) + 10 \log_{10}\left(\frac{4S}{A}\right) + 3 \qquad (\mathrm{dB}) \tag{1.15}$$

where

A is absorption area defined as $A = \frac{V}{6T}$ (m^2 Sabine)

L_{p} is noise level in room (dB re 20 μPa)

$L_{\mathrm{v(ref\ 50\ nm/s)}}$ is vibration level in (dB)

S is the area of the radiation surface (m^2).

Rivas model

Rivas model [23] is a European project that ended in 2013 focusing on the assessment of mitigation measures to reduce ground vibrations and ground-borne noise, and the associated annoyance reduction by railway lines. The model provided 1/3-octave response spectra in the frequency range of 4–250 Hz. Four transfer functions are applied to estimate building vibration and resulting in ground-borne noise, as follows.

1. TF1 is the transfer function from the ground near the tracks, 8 m from the track center in RIVAS, to the free field ground near the building
2. TF2 is the transfer function from the ground (near building) to the building foundations
3. TF3 is the transfer function from the building foundations to the floor
4. TF4 is the transfer function from floor vibration to room ground-borne noise.

Transfer from reference distance to ground near the building, TF1
Six transfer functions from the ground near the track (8 m from the track center) to the ground near the building (12, 16, 20, 24, 28 and 32 m from the track center) were calculated with a 2.5 D BEM (Boundary Element Method) for each soil type. Three different sites were considered in RIVAS:

- Homogeneous ($C_S \sim 250$ m/s)
- Layered with increasing stiffness (from $C_S \sim 130$ m/s to $C_S \sim 350$ m/s)
- Soft soil ($C_S \sim 130$ m/s).

Transfer from Ground to Building Foundations, TF2
The empirical model Vibra-2 [33] was used to calculate TF2 corresponding to the insertion loss of the building. As a result in the frequency range 4–250 Hz, the average value of relative vibration response increased at the starting point (4 Hz) by 1 dB when transmitting from foundation to floor, then decreased gradually to around -11 dB at 30–63 Hz, and after that went up to almost 0 dB at 250 Hz. A standard deviation of 5 dB was assumed due to the lack of information. An additional result was that softer soils or shallower foundations gave smaller attenuation from ground to building foundations.

Transfer from Building Foundations to Floor, TF3
Concrete and wood floors are considered to calculate transfer from building foundations to the floor. To calculate average values for typical floors, the empirical model Vibra-2 was used.

Transfer from Floor Vibration to Room Ground Borne Noise, TF4

The following transfer function TF4 was used to calculate the space averaged sound level $L_{\mathrm{P(av)}}$ from the vibration level at mid-span $L_{\mathrm{v(meas)}}$. It is assumed that the floor space average velocity is lower than the mid-span velocity, and the space averaged room noise is higher than the noise at the room center, considering both floor and ceiling radiation and neglecting walls. Based on the results, the relative response (TF4) in the frequency range 16 to 61 Hz was higher than at other frequencies such that it reached a peak of 25 dB at around 30 Hz. A simplified formula is presented below:

$$L_{\mathrm{P(av)}} \approx L_{\mathrm{v(meas)}} + 7 \qquad \text{(dB)}. \tag{1.16}$$

The sound pressure level reference is 20 μPa and the velocity level reference is 5 nm/s.

HS2 model

The High Speed 2 (HS2) model [34] is developed based on a validated ground vibration prediction model for the UK called HS1 [35]. The HS1 model was empirically developed by analyzing over 3,000 measurements at speeds of up to 300 km/h.

The HS2 model focuses on vibration caused by trains at speeds up to 360 km/h at the frequency range of 16–250 Hz in 1/3-octave bands. According to this model, by assuming that the effective roughness of rail and wheel is the only speed-dependent term, the vibration spectrum, $L_{\mathrm{v2,rms}}$, for a train speed v_2 can be estimated by the scaled vibration spectrum at train speed v_1, formulated as follows.

$$L_{\mathrm{v2,rms}}(f) = L_{\mathrm{v1,rms}}(f) + R_{\mathrm{eff}}(\lambda, \mathrm{v}_2) - R_{\mathrm{eff}}(\lambda, \mathrm{v}_1) \tag{1.17}$$

$$R_{\mathrm{eff}}(\lambda) = 10 \log_{10} \left(10^{R(\lambda)/10} + \sum_{K} 10^{L_{\mathrm{K}}(\lambda)/10} \right) \tag{1.18}$$

$$L_{\mathrm{K}}(\lambda) = R(\delta_{\mathrm{K}}) + A - \left(\frac{\log_{10} \lambda - \log_{10} \delta_{\mathrm{K}}}{B} \right)^2 \tag{1.19}$$

where,

f is the frequency (center frequency of a frequency band) under consideration (Hz)

$R_{\mathrm{eff}}(\lambda, \mathrm{v})$ is the effective roughness in dB representing the displacement amplitude resulting from wheel-rail interaction at the wheel-rail interface at train speed v (m/s) and roughness wavelength λ (m)

A and B are constants defining the amplitude and width of the parabolic term

δ_{K} is the K^{th} sleeper or axle pitch

$L_{\mathrm{K}}(\lambda)$ is the vibration level due to the K^{th} sleeper and axle passage frequency.

To calculate sound pressure levels (L_{pASmax}) generated by floor vibration in the room, the equation proposed by Bolt Beranek and Newman / Kurzweil [36] is used.

1.6 Summary of model types and limitations

Generally speaking, most engineering prediction models are based on multiplications of factors (physical quantities) assumed to be independent or an equivalent summation of terms (dB-scale). These terms describe vehicle type, vehicle speed, track type and condition, ground properties, propagation distance in the ground, coupling of vibrations between ground and building foundation, coupling of vibrations between building foundation to, primarily, floors and ceilings, and the relation between vibrations of floors and walls and the sound pressure level in the room due to sound radiation. In some models, several of these factors are joined to a single one that is determined from experimental investigations.

In many existing models, the methodology and models do not take into consideration the statistical variation of the source and wave propagation. Ignoring uncertainty in a ground-borne noise prediction model can lead to inaccurate noise level estimations, potentially underestimating risks, and resulting in financial issues. Although some models consider safety factors to handle this issue, statistical approaches are still needed to consider uncertainties in propagation paths and different frequency bands.

1.7 Outline

This thesis is structured as follows:

Chapter 2 describes the various measurement setups and measurement locations used in this project. The chapter also presents the numerical simulations conducted in this study.

Chapter 3 presents an analysis of measurement data. It includes discussions of source terms, wave propagation, and transfer functions to determine how the propagation path affects vibration levels. Additionally, a brief overview of numerical analysis results is included.

Part II, the appended paper, provides a detailed analysis of the numerical work.

Part III, the appended report, presents a developed model and methodology for ground-borne noise prediction in Swedish Transport Administration projects based on the measurement results in Chapter 3.

CHAPTER 2

Methods

2.1 Introduction

In this study, a ground-borne noise model is developed using existing knowledge, measurements, and numerical simulations. For the development of the model, measurements and numerical analyses have been carried out. Measurements were conducted in several locations. 1) In the Gårda tunnel and in two houses situated directly above it, measurements were used to calculate vibration levels and transfer functions. 2) Moreover, decay measurements were performed on the ground surface above the Gårda tunnel to gain insights into attenuation patterns. 3) Finally, measurements were conducted in a house at Övre Fogelbergsgatan 1 to estimate how vibration level changes when traveling through the floors. Furthermore, to improve the accuracy of the model, measurements obtained from the Åsa tunnel were incorporated. Notably, the Håknäs speed correction method was also employed to estimate speed correction in the development model. A numerical calculation was also performed to determine how the vibration levels change with position in the tunnel. Following are detailed descriptions of these measurements and numerical calculations.

2.2 Measurements

2.2.1 The Gårda tunnel measurements

Vibration measurements were conducted in the Gårda tunnel. A large number of apartment buildings and villas are located above the tunnel. The Gårda tunnel is a 2,163 m long railway tunnel in Göteborg, Sweden. It stretches between Gubbero in the north and Almedal in the south, along the West Coast Line. The tunnel is double-track and built in bedrock. The Gårda tunnel is a blasted track of old Swedish standards. According to old standards [37], the thickness of the ballast and sub-ballast layers in the Gårda tunnel is estimated to be approximately 0.8 meters. The sleepers within the tunnel are made of wood.

To collect data, different types of accelerometers and seismometers were applied to the tunnel wall and sleepers. Four positions are defined on both the tunnel wall and the sleepers in order to measure vibrations with good coverage. Positions are named from 1 to 4, ordered from north to south.

Figure 2.1 shows the accelerometer position on the sleeper. Tri-axle Dytran accelerometers model 3143d were mounted in four positions on the sleepers measuring in three directions (vertical, horizontal parallel to the track, and horizontal normal to the track). Distance between the first and second positions on the sleeper is 8.2 m; between the second and third positions, it is 8.4 m; and between the third and fourth positions, it is 14.3 m.

Figure 2.1: Accelerometer position on the sleeper.

Both Dytran accelerometers and Dytran seismometers are used for measuring vibrations along the tunnel walls. Tri-axle accelerometers were positioned at all locations on the tunnel wall. For measurement positions 2 and 3, seismometers were attached in both horizontal (normal to the tunnel wall) and vertical directions using aluminum cubes attached firmly to the bedrock by bolts. In positions 1 and 4, seismometers were only mounted horizontally to

capture vibrations perpendicular to the tunnel wall (See Figure 2.2). Information about tunnel wall measurement positions and transducer models is presented in Table 2.1. Regarding tunnel wall measurement positions, the distance between the first and second positions is 10.3 m; between the second and third positions, it is 4.7 m; and between the third and fourth positions, it is 17.7 m.

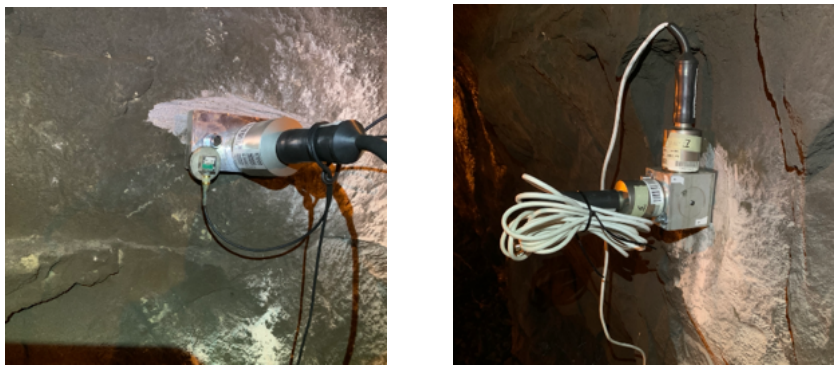

(a) (b)

Figure 2.2: Measured locations on the tunnel wall in the Gårda tunnel: (a) positions 1 and 4 with one seismometer, (b) positions 2 and 3 with two seismometers.

Table 2.1: Transducer positions on the tunnel wall. x denotes the vertical direction, y represents the horizontal direction parallel to the wall, and z represents the horizontal direction perpendicular to the wall.

Position	Model	Direction	Height above rail head (m)	Distance to track center (m)
position 1	Accelerometer 3293A Seismometer 3191a1	xyz z	1.75	2.75
position 2	Accelerometer 3293A seismometer 3191a1	xyz xz	1.25	2.75
position 3	Accelerometer 3293A seismometer 3191a1	xyz xz	1.35	2.75
position 4	Accelerometer 3293A seismometer 3191a1	xyz z	1.15	2.75

In order to measure train speed, a speed radar was set up on a stand close to position 4 where the view was clear for capturing data. The radar captured both north and south pass trains. The highest measured train speed was around 110 km/h.

The measurements were carried out approximately mid-length in the Gårda tunnel over three days, from 27th to 30th March 2021. A total of 930 train passages were registered from 2021-04-27 at 04:20:00 to 2021-04-30 at 23:55:00.

Train types were X61, X31, X55, X14, X12, X11, X29, X52, and different kinds of freight trains. Most of the passages were related to X61, X31, X55, and freight trains. Other train types were not considered in the analysis due to their limited number. About 450 of the passages were along the track closest to where the vibration measurements were taken. Table 2.2 shows the properties of the passenger trains of interest based on Figure 2.3.

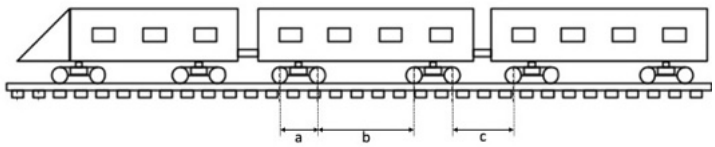

Figure 2.3: Train dimensions. Adapted from reference [12].

Table 2.2: Train dimension values [12].

Train model	Length (m)	Weight (kg)	Bogie distances (m)		
			a	b	c
X55	107.2	228	2.7	16.3	4.9
X61	74.3	154	2.7	16.3	4.8
ETS (X31)	78.9	153	2.7	16.3	4.125

Measurement of sound pressure and vibration in the room

Sound and vibration measurements were conducted inside two houses above the tunnel, at addresses Prospect Hillgatan 10 and Carlbergsgatan 13, see Figure 2.4. Prospect Hillgatan 10 is approximately 55 m above the tunnel floor, while Carlbergsgatan 13 is around 40 m above the tunnel floor. The tunnel ceiling is approximately 9 meters above the tunnel floor based on the Göteborg map data. The measurements in the houses were performed simultaneously with the tunnel measurements. The measurements at Prospect Hillgatan 10 were conducted from April 27, 2021, at 04:20:00, to March 28, 2021, at 09:00:00. Measurements at Carlbergsgatan 13 were carried out from April 28, 2021, at 12:30:00, to March 30, 2021, at 23:55:00. At Prospect Hillgatan 10, transducers were mounted inside a 2.5 m $\times$ 2.5 m $\times$ 2.5 m bedroom where train noise was clearly audible. The floor covering was parquet inside the room. At Carlbergsgatan 13, a storage room was chosen on the ground floor without any floor cover, with a dimension of 1.5 m $\times$ 4 m $\times$ 2.3 m.

The house measurements included one microphone placed in the corner, one seismometer (Wilcoxon model 731) positioned on the floor recording vertical

direction, and one tri-axle accelerometer (Dytran, model 3293A) mounted on the wall. Two seismometers (Wilcoxon model 731) and one tri-axle accelerometer (Dytran model 3293A) were mounted on the foundation. Seismometers on the foundation capture vibration in two directions: vertical and horizontal (normal to the foundation). Figures 2.5 and 2.6 show sensor positions in the two houses.

Moreover, a speaker and two microphones were used to calculate the transfer function from sound in the corner of the room to the average sound at the room center. One microphone was positioned in the corner of the room, the other was moved around the room center to measure the emitted noise from the speaker.

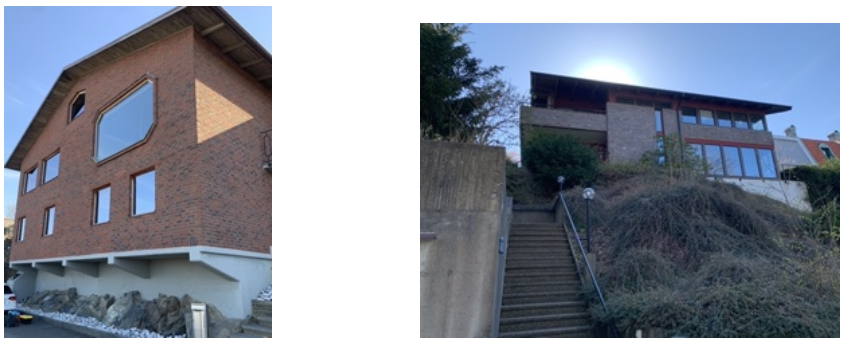

(a) (b)

Figure 2.4: Measured locations above the tunnel: (a) Prospect Hillgatan 10, (b) Carlbergsgatan 13.

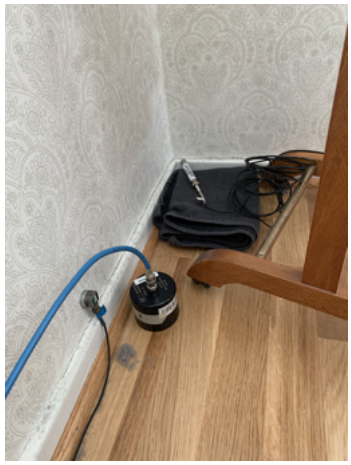

(a)

(b)

Figure 2.5: Measured locations at Prospect Hillgatan 10: (a) inside the room, (b) on the foundation.

(a)

(b)

Figure 2.6: Measured locations at Carlbergsgatan 13: (a) inside the room, (b) on the foundation.

Decay measurements on the ground surface

Measurements were carried out on the ground surface above the Gårda tunnel at the yard of Prospect Hillgatan 10 to investigate distance attenuation. The measurements carried out on September 2nd, 2021, started at 13:38:03 and lasted until 15:18:46.

As shown in Figure 2.7, measurement points extended perpendicular to the

tunnel from R0 to A6. Receivers were placed along a line of about 40m, using a spatial resolution of around 6 m starting from above the tunnel (R0 which is on the foundation). In all positions, seismometers (Wilcoxon model 731) were located to capture vertical direction (perpendicular to the ground surface). In addition, three tri-axle accelerators (Dytran model 3293A) were placed at positions A3, A5, and A6 to compare with the data recorded by the seismometers. The transducers captured valid signals from only 10 train passages.

Figure 2.7: Location for decay measurements on the ground surface above the Gårda tunnel.

Floor-to-floor decay Measurements

In order to determine how the vibration changes when transferred from one floor to another, measurements were taken in Övre Fogelbergsgatan 1 on March 9th, 2022 from 10:00:00 to 11:30:00. Övre Fogelbergsgatan 1 is a place located above the Västlänken tunnel, currently under construction in Göteborg city. The building has ten floors, and its foundation is on the bedrock. Seismometers (Dytran model 3191a1) were mounted outside the building, at the entrance, on floors 4, 7, and 10 in the vertical direction. The hydraulic hammer applied during construction in the Västlänken tunnel was used as a source for these measurements. The hydraulic hammer was operated only once during the measurement period so that vibrations could be recorded on all floors.

(a)

(b)

Figure 2.8: Example of sensor positions in Övre Fogelbergsgatan 1: (a) outside the house, (b) on floor 4.

2.2.2 The Åsa tunnel measurements

Data from previous measurements in the Åsa tunnel are also used as input to the model and model development. According to the Åsatunnel report [38], vibrations were measured on the tunnel wall in both vertical and horizontal directions in the Åsa tunnel on the Västkustbanan from 2019-11-21 to 2019-12-23. Vibrations have been measured for 2683 passages during this time. The Åsa tunnel has a track with ballast and sub-ballast. The thickness of the ballast layer is 50 cm and the thickness of the sub-ballast is 80 cm. The train types passing through the Åsa tunnel are freight trains, X61, X 55, X31, and X 2000. The highest measured train speed is 196 km/h.

2.2.3 The Håknäs tunnel measurements

In this project, the speed correction model presented by the Håknäs tunnel report [39] is used. According to the Håknäs tunnel report, the track inside the tunnel is built with a thick sub-ballast of 1.6 m and a ballast of 0.5 m. The track was recently constructed, and a new rail was installed. Measurements were taken at different positions: on the sleeper (vertical), on the tunnel wall (horizontal, perpendicular to the track), and above the tunnel. The measurements were made with Regina trains at speeds of 120-280 km/h. The numerical tool Findwave was used to predict speeds up to 400 km/h using a model for the Citytunneln in Malmö. The vibration level was evaluated at the

maximum level for the time-weighting Slow during the passage. The speed dependence model is presented as follows:

$$\Delta L_{\mathrm{S}} = 20 \log_{10} \frac{v}{v_{\mathrm{ref}}} \quad \text{for 80–160 km/h} \tag{2.1}$$

$$\Delta L_{\mathrm{S}} = 10 \log_{10} \frac{v}{v_{\mathrm{ref}}} \quad \text{for 160–240 km/h} \tag{2.2}$$

$$\Delta L_{\mathrm{S}} = 18 \log_{10} \frac{v}{v_{\mathrm{ref}}} \quad \text{for 240–320 km/h} \tag{2.3}$$

$$\Delta L_{\mathrm{S}} = 0, \quad \text{i.e. constant, above 320 km/h} \tag{2.4}$$

where ΔL_{S} is the speed correction term, v is the train speed of interest, and v_{ref} is the reference speed at which the source term was determined.

2.3 Estimated model uncertainty

The uncertainty of the predicted ground-borne noise level is estimated following [40] via a sum of variances of the model terms

$$u_c^2 = \sum u_i^2$$

where u_c is the combined standard uncertainty and u_i^2 is the variance of model term i, assuming that the uncertainty of the predicted level can be described by a normal distribution. The use of two standard deviations (i.e. $2u_c$) is suggested here, defining an interval with a confidence level of approximately 95%.

2.4 Numerical simulations of wave propagation from tunnels

The finite element method (FEM) has been used to model wave propagation and resulting vibration amplitudes in a lightly damped elastic medium, modeling bedrock, when excited by forces up to 1 kHz. An underground tunnel is modeled in 2D and 3D in half and full space, see Figure 2.9. The ground type modeled is bedrock typical for Swedish ground conditions. In our simulation, the bedrock has a Young's modulus of 50 GPa, a density of 2400 kg/m^3, a Poisson ratio of 0.3 and a damping ratio of 0.008. The elastic medium is homogeneous and isotropic, i.e., no effects of cracks are included. The Structural Mechanics Module of COMSOL Multiphysics software and its Solid Mechanics interface in the frequency domain is used to calculate the velocity response due to a unit force. A low reflection boundary is used at the boundaries to

simulate the infinite extension of the domain. The boundary condition is an impedance matching strategy using an impedance of $\rho\ (c_p + c_s)/2$, where c_p is the speed of P-waves, c_s is the speed of S-waves and ρ is the density of the bedrock in which the waves propagate.

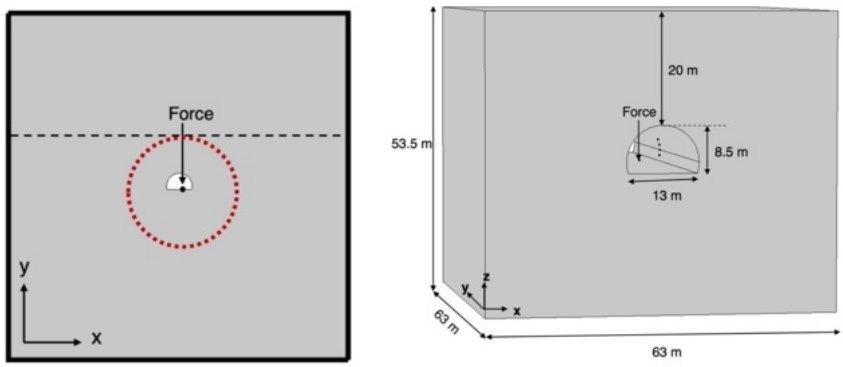

(a) (b)

Figure 2.9: Geometrical layouts of the study: (a) 2D model where the dashed line indicates the free surface in the half-space case, (b) 3D model.

CHAPTER 3

Results

3.1 Introduction

In this chapter, the data collected from the measurement sites described in Chapter 2 are analyzed step by step to find a source strength and determine how the propagation path affects vibration levels. Additionally, finite element analysis and the result of the tunnel shielding effect are expressed.

3.2 Measurement results

3.2.1 Analysis

The analysis made here is based on the Gårda and Åsa tunnel measurements and the Håknäs speed correction model. The model is developed using time-weighting Slow rather than time-weighting Fast for several reasons. 1) A significant number of models and datasets are available utilizing time-weighting Slow; 2) time-weighting Slow results in more stable transfer functions. Conversely, according to our investigations, when time-weighting Fast is used, the results have a larger statistical spread. Therefore, we used time-weighting Slow to predict the ground-borne noise model. However, sound pressure levels inside the rooms were calculated in time-weighting Fast for comparison with the final results in time-weighting Slow (Part III, Section 3.12).

In the following, the analysis is made in 1/3-octave bands, for both equivalent level and maximum level with time-weighting Slow. To calculate the

level with time-weighting Slow, the following process is carried out: band-pass filtering is applied at frequencies with acceptable signal-to-noise ratio, here higher than 6 dB; integration from vibration acceleration to velocity; applying A-weighting using time-domain filtering; averaging in the 1-second window using simplified filtering (moving average with constant filter coefficient is used), finding the maximum level; and calculating the 1/3 octave band spectrum for the 1-second interval of the maximum level.

3.2.2 The Gårda tunnel measurement results

Validity check

In the Gårda tunnel measurements, transducers were placed at several locations to determine if they captured valid data, see Section 2.2.1. Signal quality assessment is investigated by comparing vibrations in the time domain and frequency domain at different measurement points. Figures 3.1 show an analysis of four positions on the sleeper in the time and frequency domain when a freight train passes through the tunnel. According to the figure, the signal from the transducer in position 4 on the sleeper is very low, and it does not capture the vibrations correctly. The chosen sleeper may have been damaged by loose wood or the transducer may not have been mounted firmly enough on the sleeper. In general, for tunnels, it is often more common and convenient to measure vibrations on the tunnel wall. Therefore, the tunnel wall is used as the reference distance rather than the sleeper for calculating the source term in this study.

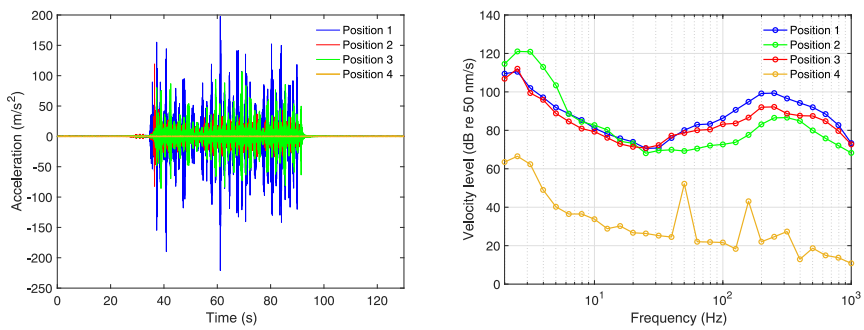

(a) (b)

Figure 3.1: Vibration in the time and frequency domain for the sleeper in the vertical direction: (a) in the time domain, (b) in the frequency domain.

Figure 3.2 demonstrates results related to the accelerometer on the tunnel wall in the vertical direction. According to Figure 3.2(b), transducers located

at positions 1 and 4 show peaks at 50 Hz. The frequency component at 50 Hz is related to the characteristics of the electrical power system. Additionally, based on the time-domain figure, the vibration amplitude in position 1 is significantly higher than in the other positions during the initial part of the passage. Position 2 seems to show reasonable results. However, the seismometers performed better than the accelerometers. The signal-to-noise ratio was significantly higher for the seismometers at lower frequencies (below 100 Hz). No qualified signals were captured by the accelerometers inside the houses due to low signal-to-noise. As a result, only seismometer records were used in further analysis for the development of the prediction model.

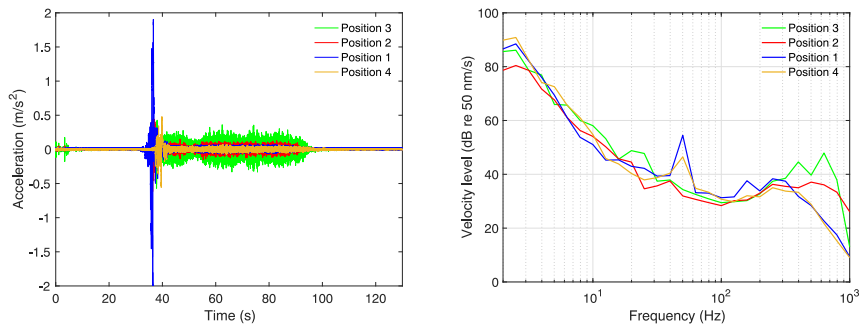

(a) (b)

Figure 3.2: Vibration related to accelerometers in the time and frequency domain for the tunnel wall in the vertical direction: (a) in the time domain, (b) in the frequency domain.

Figures 3.3 and 3.4 show vibration captured by seismometers in vertical and horizontal directions on the tunnel wall. Figures show that transducers in all positions on the tunnel wall in the horizontal and vertical directions captured the signal effectively. According to both figures, results at position 3 on the tunnel wall in both vertical and horizontal directions differ from those at other positions, especially at lower frequencies. Based on these observations, our focus will be on positions 1, 2, and 4 for horizontal direction and position 2 for vertical direction on the tunnel wall, as they have shown consistent and reliable data capture in the frequency range of interest.

Comparing vibrations in different directions on tunnel wall

As found in the "Validity check" section, the signals obtained from the transducer mounted on the tunnel wall at position 2 will be utilized for the analysis in the vertical direction. The vibration level for both vertical and horizontal directions in position 2 is considered to compare level differences in two di-

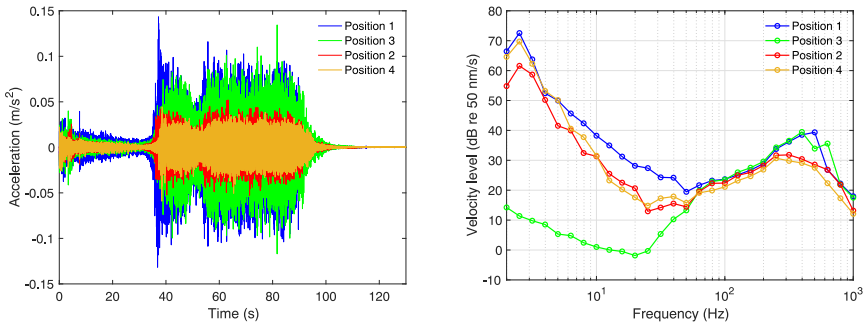

(a) (b)

Figure 3.3: Vibration related to seismometers in the time and frequency domain for the tunnel wall in the horizontal direction: (a) in the time domain, (b) in the frequency domain.

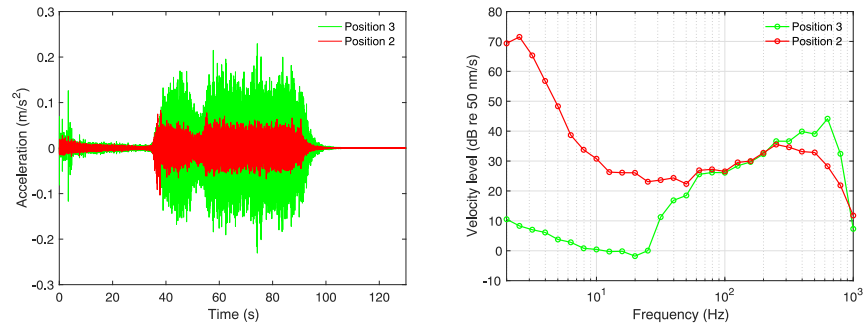

(a) (b)

Figure 3.4: Vibration related to seismometers in the time and frequency domain for the tunnel wall in the vertical direction: (a) in the time domain, (b) in the frequency domain.

rections. Based on our investigation vibration level in the vertical direction is higher than the horizontal direction on the tunnel wall. Figure 3.5 is an example of one passage in the tunnel. According to the figure, the vertical direction (x) shows higher vibration levels than the horizontal direction (z) in both accelerometer and seismometer records. The legend's notation, "2x" and "2z", indicates that the results correspond to position 2 on the tunnel wall in x and z directions. In the analysis, we consider both directions.

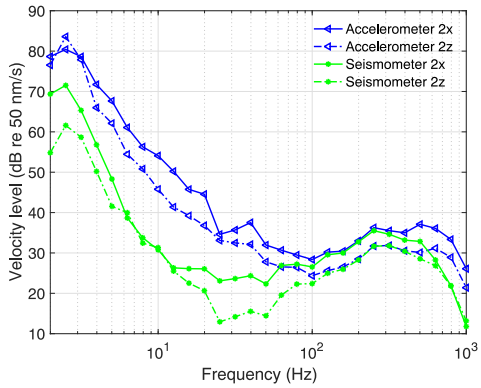

Figure 3.5: Vibration level related to one passage on the tunnel wall in vertical and horizontal directions for both accelerometer and seismometer.

Train speed effect

The maximum train speed passing through the Gårda tunnel was 110 km/h during the measurements. Data from the Åsa tunnel, which includes measurements at higher train speeds (maximum speed of 196 km/h), is used in the analysis. This decision is made due to fewer passages and the lack of high-speed passages in the Gårda tunnel.

Two types of trains are considered to determine the effect of train speed on vibration levels: freight trains and passenger trains. The number of train passages and the related speed range used in this study is given in Table 3.1.

Table 3.1: Number of train passages.

Tunnel name	Number of trains		Train speed range (km/h)	
	Freight	Passenger	Freight	Passenger
The Gårda tunnel	18	220	18–60	43–110
The Åsa tunnel	400	1740	60–1116	120–196

The effect of different train speeds on the maximum vibration level along the tunnel wall is considered to estimate the speed correction term. Figure 3.6 shows the maximum vibration level, L_{vASmax}, versus train speed on the tunnel wall in the vertical direction. The results are related to trains passing through both the Gårda and the Åsa tunnel measurements presented in Table 3.1.

Figure 3.6 also shows a linear regression fitted on data sets for each type of train. For each line, the slope, m, and the coefficient of determination, R^2, are calculated and shown in the figure. m is defined using Eq 3.2.

$$L_{\mathrm{vASmax}} = m \times 20 \log 10 \left(\frac{S}{S_{ref}} \right) \tag{3.1}$$

where S is the speed of each train, and S_{ref} is the reference speed. In this study, four reference speeds are considered for each train type in each tunnel: 160 km/h for passenger trains and 90 km/h for freight trains in the Åsa tunnel; 80 km/h for passenger trains and 50 km/h for freight trains in the Gårda tunnel. In general, the closer the reference speed is to the speed of calculation, the higher accuracy is expected. For small relative speed differences, the assumed speed dependence has a minimal influence on the final result, and speed adjustment may be omitted, leading to more reliable results.

R^2 is defined as below:

$$R^2 = 1 - \frac{SS_{\mathrm{res}}}{SS_{\mathrm{tot}}} \tag{3.2}$$

where SS_{res} is the sum of squared differences between the observed values and the predicted values from the regression line and SS_{tot} is the sum of squared differences between the observed values and the mean of the dependent variable. The R^2 value range is between 0 and 1. When the modeled value and observed value are exactly the same, the R^2 is equal to 1.

Figure 3.6(b) shows a low value of R^2 for the Åsa tunnel. That means using the line fit as a prediction model would be linked with large uncertainty. Based on Figure 3.6(a), since there are only a limited number of data points available for freight trains, the calculated m value is not reliable. The highest value of R^2 corresponds to passenger trains in the Gårda tunnel with an m value of 1.15. This m value is close to the value of 1 found in the Håknäs speed correction model (Eq 2.1).

Estimating consistent m values for the Gårda and Åsa tunnels based on the obtained results is challenging. This challenge arises particularly at higher train speeds due to the low value of R^2 (high uncertainty) observed in the Åsa tunnel results. Consequently, it is more reasonable to use the existing Håknäs speed correction model, which is based on Regina trains and covers train speeds from 80 km/h to higher than 320 km/h.
The Håknäs speed correction model (Eq. 2.1 to Eq. 2.4) is used in our prediction to scale the single vibration level value. The HS2 model is used for spectrum scaling according to Eq 1.19 to 1.17. Section 3.5 of Part III describes how HS2 speed correction is used in the prediction model.

The vibration level is reproduced on the tunnel wall in the Gårda and Åsa tunnel for passenger and freight trains using Eq. 2.1 to Eq. 2.4 to double-check how well the Håknäs speed correction model works for our model. Firstly, the maximum vibration level is calculated on the tunnel wall for each passage, and then, the Håknäs speed correction model is applied to estimate the source

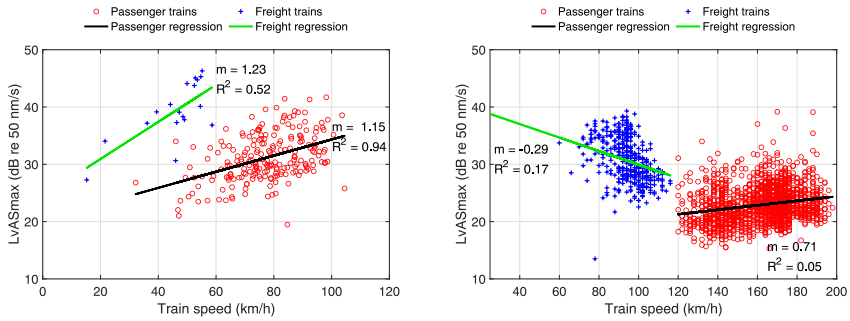

Figure 3.6: Maximum vibration level versus train speed on the tunnel wall in the vertical direction and the regression line for each train type: (a) in the Gårda tunnel, (b) in the Åsa tunnel.

strength of each train type for each tunnel. Secondly, the arithmetic average and the standard deviation (STD) of the source strength are calculated for each train type in each tunnel. Thirdly, the Håknäs speed correction model is added to the average of source strength, the average plus STD, the average plus two times STD, and the average plus three times STD. Predicted and calculated L_{vASmax} versus train speed is shown in Figure 3.7 for different train categories in each tunnel. Lines show the predicted model and dots show calculated L_{vASmax} in each tunnel for different train passages. According to the figure, the reproduced model using the Håknäs speed correction model plus two times standard deviation covers all passages in the Gårda tunnel. In the Åsa tunnel, this model (average of source term plus 2STD) represents all freight trains and covers approximately 95 % of the passenger trains.

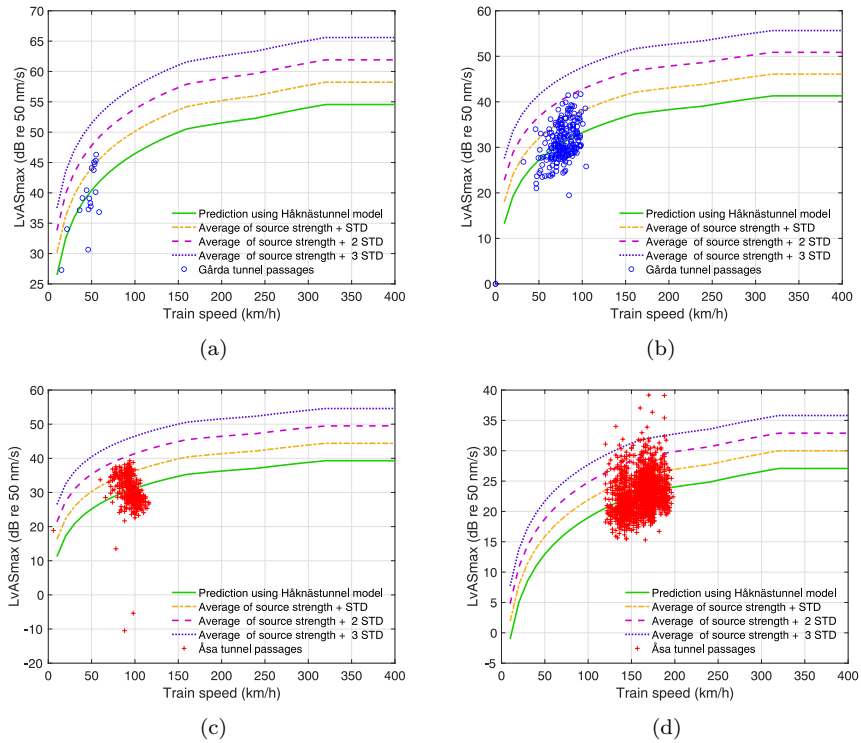

Figure 3.7: Reproduced vibration level on the tunnel wall using the Håknäs speed correction model in average, average plus one standard deviation (STD), average plus two STD, and average plus three STD: (a) freight train in the Gårda tunnel, (b) passenger train in the Gårda tunnel, (c) freight train in the Åsa tunnel, (d) passenger train in the Åsa tunnel.

The effect of track type

The prediction model utilizes measurements from the Åsa tunnel to estimate the source term for new ballasted tracks and also suggests a source term based on Gårda measurements for older ballasted tracks, (See Part III, Section 3.4). Untreated ballasted tracks are used as the reference track in the prediction model. An analysis of the source strength in maximum level is made for each train type in two tunnels to assess the impact of ballasted track types on vibration level. To do this, the maximum level of source strength related to each passage is calculated using the HS2 speed correction model in the vertical direction on the tunnel wall (As mentioned in Section "Train speed effect", the HS2 model is used as the speed correction for spectrum analysis). Afterward, an arithmetic average is calculated based on multiple passages of each train type. The comparison between the results from both tunnels is displayed in

Figure 3.8. The red dash-dotted lines show the Gårda tunnel source terms adjusted to the Åsa tunnel reference speed. Green solid lines depict the source term of the Gårda tunnel adjusted to the Gårda reference speed (80 km/h for passenger train and 50 km/h for freight train), and blue dashed lines show the source term of the Åsa tunnel at its own reference speed (160 km/h for passenger train and 90 km/h for freight train). The number of train passages in the Gårda and Åsa tunnel and their related speed range are presented in Tables 3.2 and Table 3.3 respectively.

According to Figure 3.8, in general, the vibration levels related to the Gårda tunnel are higher than those for the Åsa tunnel for all train types. It can be explained by the fact that the Gårda tunnel is an older track than the Åsa tunnel. The results from the Åsa tunnel show an unreasonable increase and jump in level when frequencies exceed 630 Hz. This sudden change could be linked to issues with how the transducers were mounted or positioned during the measurements. Additionally, the results from the Åsa tunnel and the Gårda tunnel (re $S_{ref,\text{Å}sa}$) follow the same trend at frequencies around 40 to 400 Hz for passenger trains and around 30 to 630 Hz for freight trains. However, there are differences, at lower frequencies and higher frequencies for some train types. These differences could be attributed to different ballast thicknesses in both tunnels, different types of sleepers, and a higher train speed range in the Åsa tunnel than the Gårda tunnel. Furthermore, as evident from the figures, the source term in the Gårda tunnel experiences less variation when adjusted to its own reference speed compared to the Gårda results adjusted to the Åsa reference speed. Therefore, a reference speed closer to the interested speed range results in a more stable source term outcome.

Table 3.2: Number of train passages in the Gårda tunnel and in the Åsa tunnel.

Tunnel name	Number of trains			
	Freight	X55	X61	ETS (X31)
The Gårda tunnel	18	10	155	66
The Åsa tunnel	400	330	140	1300

Table 3.3: Speed ranges related to train passages mentioned in Table 3.2.

Tunnel name	Speed range (Km/h)			
	Freight	X55	X61	ETS (X31)
The Gårda tunnel	18–60	60–94	47–110	32–103
The Åsa tunnel	60–116	122–196	120–184	120–196

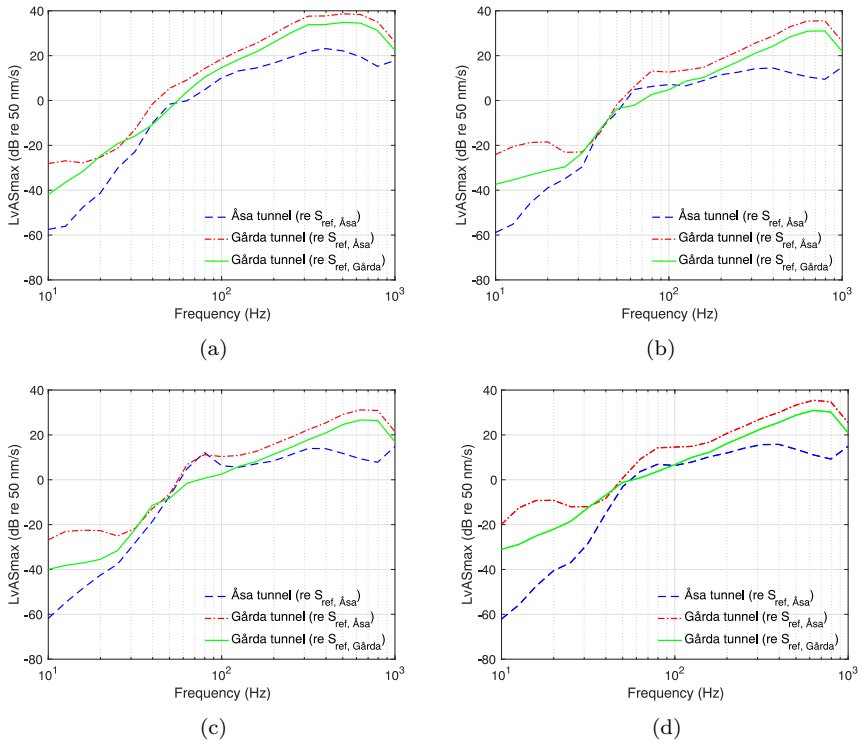

Figure 3.8: The effect of track type on the maximum level of source strength for each train type: (a) Freight train, (b) X55, (c) X61, (d) ETS (X31).

Train Types effect on vibration levels

Here, the effect of three types of passenger trains (i.e., X61, X55, and ETS (X31) trains) as well as freight trains is considered in maximum vibration level along the tunnel wall. Table 3.2 presents the number of different train types used in this study. The maximum level of source strength for each passage on the tunnel wall is calculated using the same process explained in the previous section, "The effect of track type".

Figure 3.9 shows the maximum vibration level versus frequency on the tunnel wall in the vertical direction in separate tunnels. According to the figure, freight trains in both tunnels have higher vibration levels than passenger trains above almost 70 Hz. Moreover, the three passenger train types show similar results at frequencies above 50 Hz for the Gårda tunnel and above 10 Hz for the Åsa tunnel.

As mentioned in the previous section, "The effect of track type", the results from the Åsa tunnel show an unreasonable trend when frequencies exceed

630 Hz. To address this, an extrapolation is performed in the Åsa tunnel for frequencies higher than 630 Hz. The slope of the Gårda tunnel results (Figure 3.9(a)) in this frequency range is used for the extrapolation. Therefore, a reasonable graph is obtained for the Åsa tunnel in order to calculate the single value of the maximum level and construct the source spectra in 1/3-octave bands.

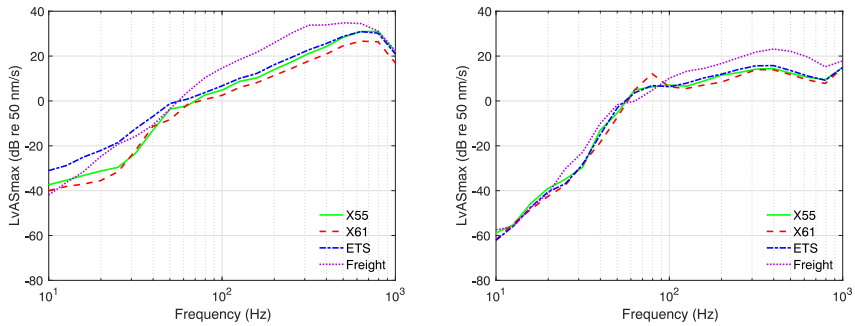

Figure 3.9: The effect of train type on maximum vibration level in the vertical direction at different frequency ranges: (a) in the Gårda tunnel, (b) in the Åsa tunnel.

Table 3.4 shows the single value of maximum level in both the Åsa tunnel and the Gårda tunnel for different train types. According to the table, the results related to three different passenger trains are close for each tunnel.

Consequently, based on the results observed in Figure 3.9 and Table 3.4, the three types of passenger trains (i.e., X61, X55, and ETS trains) can be treated as one category and freight trains as another.

Table 3.4: The average maximum value of vibration on the tunnel wall in the vertical direction in time-weighting Slow for various train types.

Train types	L_{vASmax} Gårda tunnel (dB)	L_{vASmax} Åsa tunnel (dB)
X55	34	23
ETS	34	24
X61	31	22
Freight	40	31

Propagation from tunnel wall to house

A transfer function is calculated as a function of frequency to estimate how the vibration level changes between two points. The transfer function between two points is defined as the difference in vibration level during train

passage. Here, the transfer function from the tunnel wall to Carlbergsgatan 13 and Prospekt Hillgatan 10 will be calculated, considering both vertical and horizontal directions. This analysis will encompass both the maximum and equivalent vibration levels generated by freight and passenger trains. Signal-to-noise ratio calculations were initially conducted to establish valid frequency ranges for the assessment of the transfer function. The valid signal-to-noise ratio is considered to be higher than 6 dB in this study. On the tunnel wall, in both vertical and horizontal directions, noise levels stay below the signal levels within the frequency range of 1 to 1000 Hz. This is observed for both passenger and freight trains. The valid signal-to-noise ratio varies based on positions within the houses and the types of trains being considered. Table 3.5 presents the valid frequency range in different positions in the houses. The frequency ranges are valid for both the vertical and horizontal directions within the given positions.

Table 3.5: Valid frequency range inside houses for both vertical and horizontal directions.

House	Position	Valid frequency range (Hz)	
		Freight train	Passenger train
Carlbergsgatan 13	Foundation	60–400	60–250
	Floor	60–500	60–400
Prospekt Hillgatan 10	Foundation	60–600	60–500
	Floor	60–400	60–250

Figure 3.10 shows an example of experimental results related to signal-to-noise ratio and transfer function from the tunnel wall to Prospect Hillgatan 10 in the vertical direction. Figure 3.10(a) illustrates the signal-to-noise ratio on the tunnel wall and the foundation for a single freight train. From the figure, signal levels are consistently higher than noise levels at all frequency ranges for the tunnel wall. In contrast, for the foundation, the signal-to-noise ratio exceeds 6 dB within the frequency range of 60 to 600 Hz, which is considered to give valid results. Therefore, the valid frequency range for calculating an average transfer function for freight trains is assumed to be 60 to 600 Hz. Figure 3.10(b) shows the transfer function for the frequency range of interest in the vertical direction. Vibration attenuation starts at about -12 dB at 63 Hz and gradually decreases to -33 dB at 500 Hz, which means higher frequencies experience more attention than lower frequencies. The result is similar for passenger trains (Figure 3.10(c) and (d)). However, the valid frequency range is limited to 60–500 Hz.

The calculated transfer function from the tunnel wall to the building's foundation and floor at Carlbergsgatan 13 and Prospekt Hillgatan 10 are shown in

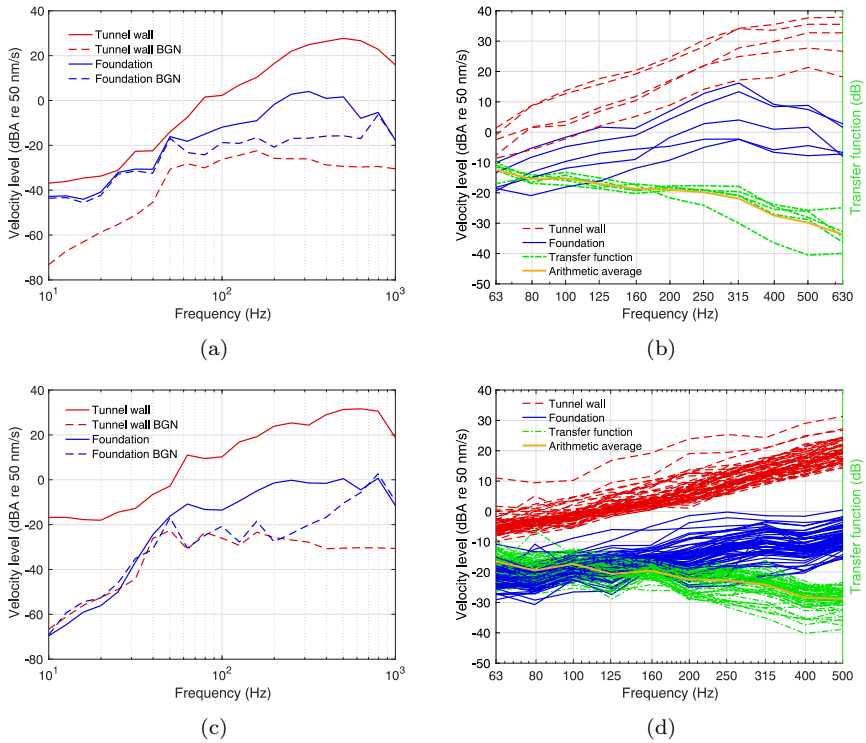

Figure 3.10: Transfer function from tunnel wall to the foundation in vertical direction at Prospect Hillgatan 10: (a) equivalent vibration levels for a single freight train with background noise (BGN), (b) transfer function for all freight train passages, (c) equivalent vibration levels for a single passenger train with background noise (BGN), (d) transfer function for all passenger trains.

Figures 3.11 and 3.12, respectively. The transfer function for both equivalent and maximum levels is presented here.

Figure 3.11 shows transmission from the tunnel wall to the building at Carlbergsgatan 13, displaying both maximum and equivalent levels for a total of six freight trains and 120 passenger trains. The transfer function is calculated from the three valid positions for the horizontal direction and one valid position for the vertical direction on the tunnel wall to the foundation and floor of the house. An arithmetic average is taken to calculate the final transfer function. As depicted in Figure 3.11(a) and (b), the transfer functions in the vertical direction demonstrate a greater vibration attenuation from the tunnel wall to the foundation in comparison to the horizontal direction. It has been also shown that vibrations at lower frequencies are less attenuated than vibra-

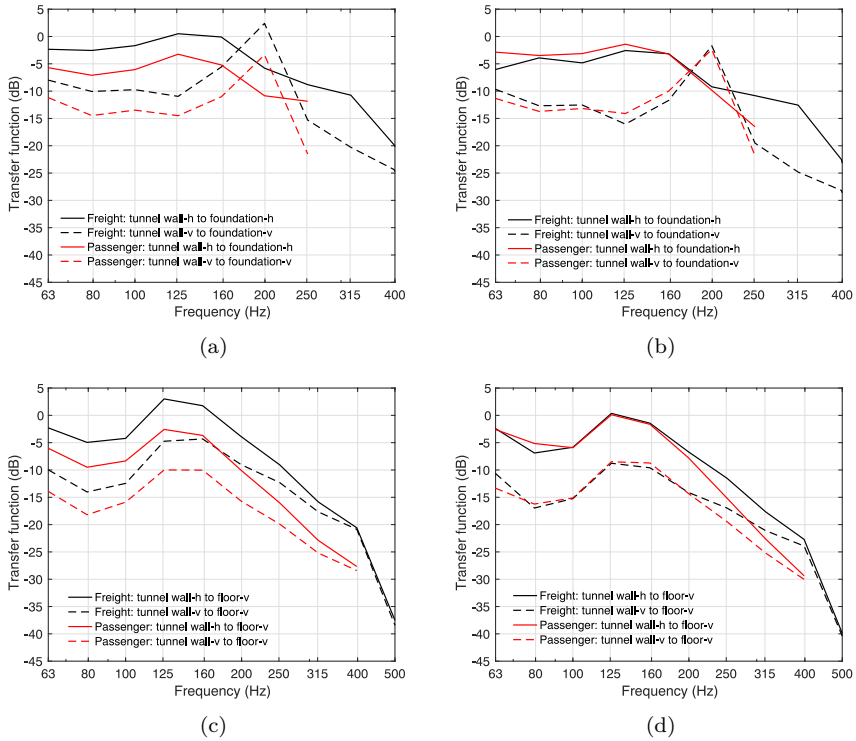

Figure 3.11: Arithmetic average of the transfer function from the tunnel wall in horizontal (-h) and vertical (-v) directions to the foundation and floor of Carlbergsgatan 13 for passenger and freight trains: (a) tunnel wall to the foundation for equivalent level, (b) tunnel wall to the foundation for maximum level, (c) tunnel wall to the house floor for equivalent level, (d) tunnel wall to the house floor for maximum level.

tions at higher frequencies. Furthermore, the results for freight and passenger trains show almost identical values at the maximum level, in contrast to the results at the equivalent level. Figures 3.11(a) and (b) show a peak at the frequency of 200 Hz on the foundation in the vertical direction at Carlbergsgatan 13. This appears for all train passages at different times as well as for the background noise. The resonance may be associated with the mounting or setup of the sensor.

Figures 3.11(c) and (d) show the transfer function from the tunnel wall to the house floor. The transfer functions follow nearly the same trend as those results related to Figures 3.11(a) and (b). However, the reduction from the tunnel wall to the floor is higher than from the tunnel wall to the foundation, mainly at the maximum level.

Figure 3.12 shows the transfer functions for maximum and equivalent levels from the tunnel wall to the building at Prospect Hillgatan 10 for 5 freight trains and 100 passenger trains. According to Figures 3.12(a) and (b), vibration levels are attenuated between the tunnel wall and foundation, identical to Carlbergsgatan 13. Figures 3.12(c) and (d) show that the vibration level from the tunnel wall in the vertical direction to the house floor in the vertical direction attenuates less than the tunnel wall in the vertical direction to the foundation in the vertical direction. Furthermore, the vibrations are amplified from the tunnel wall in the horizontal direction to the house floor in the vertical direction. The reason is that vibrations in the tunnel wall are lower in the horizontal direction than in the vertical direction. Consequently, the vertical direction provides a more accurate measure of vibration amplitude or energy.

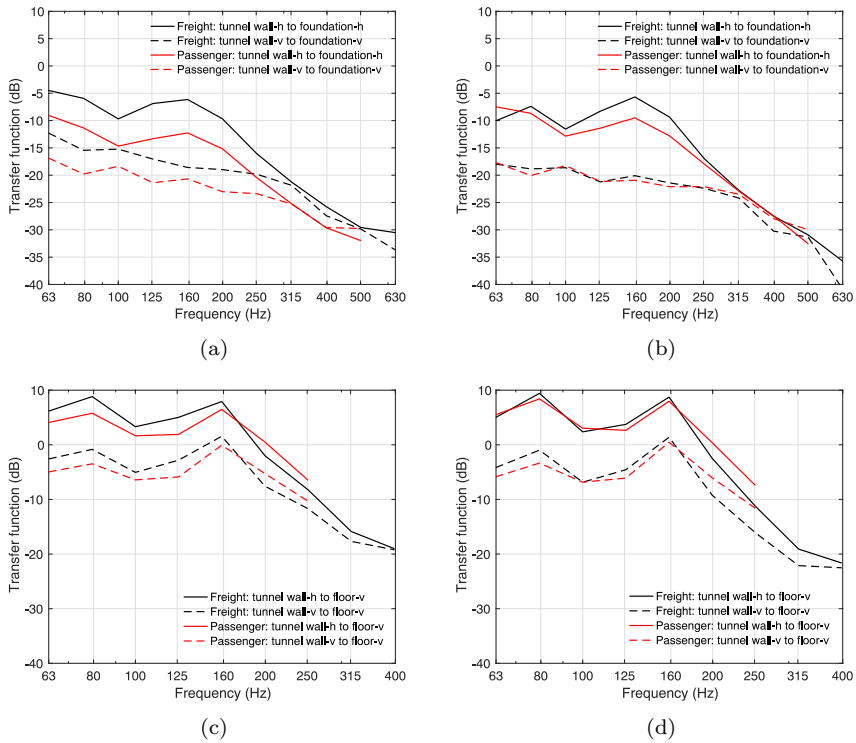

Figure 3.12: Arithmetic average of the transfer function from the tunnel wall in the horizontal (-h) and vertical (-v) directions to the foundation and floor of prospect Hillgatan 10 for passenger and freight trains: (a) tunnel wall to the foundation for equivalent level, (b) tunnel wall to the foundation for maximum level, (c) tunnel wall to the house floor for equivalent level, (d) tunnel wall to the house floor for maximum level.

Figure 3.13 shows how the vibration changes by increasing the distance from the tunnel, based on the results obtained from decay measurements for 6 passages of the trains. According to the figure, by increasing the distance from the tunnel, vibration attenuates at frequencies between around 50 to 700 Hz.

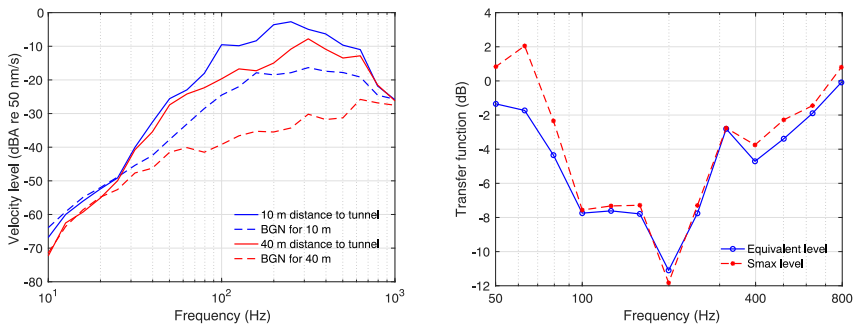

(a) (b)

Figure 3.13: Decay measurement: (a) equivalent vibration level induced by passage of a freight train at two different distances from the tunnel (10 m and 40 m), (b) the transfer function between the distances of 10 m and 40 m from the tunnel.

Coupling loss at foundation

To consider the coupling loss factor, the transfer function from the foundation to the floor is calculated for five freight trains at Prospekt Hillgatan 10 (Figure 3.15) and six freight trains at Carlbergsgatan 13 (Figure 3.14), built directly on bedrock. The transfer function is considered for frequencies with a high signal-to-noise ratio, 60-400 Hz (See Table 3.5) for both vertical and horizontal directions. As depicted in Figure 3.14, the coupling loss at Carlbergsgatan 13 remains close to 0 dB for both vertical and horizontal directions. The peak at 200 Hz in the vertical direction can be disregarded since it is attributed to background noise. On the other hand, according to Figure 3.15, the transfer function from the foundation to the house floor at Prospekt Hillgatan 10 is around 10 dB. This phenomenon can be attributed to the presence of parquet flooring on the floor of Prospekt Hillgatan 10. The resonances within the parquet floor may amplify vibrations. Therefore, the results from prospect Hillgatan 10 have been concluded to be less reliable, and only the results from Carlbergsgatan 13 have been used to estimate the coupling loss.

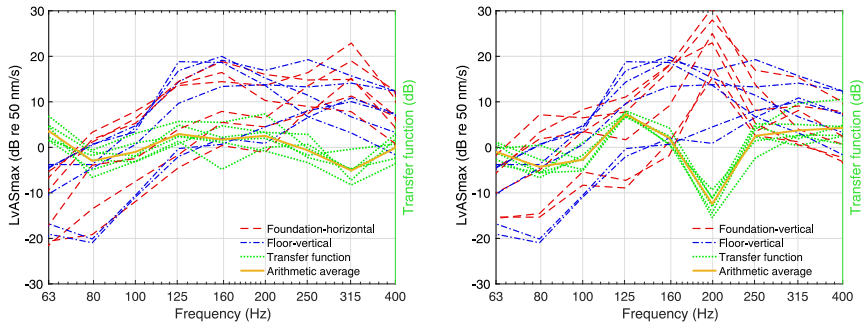

Figure 3.14: Vibration level and transfer function from foundation to floor at Carlbergsgatan 13 in vertical and horizontal directions: (a) horizontal direction, (b) vertical direction.

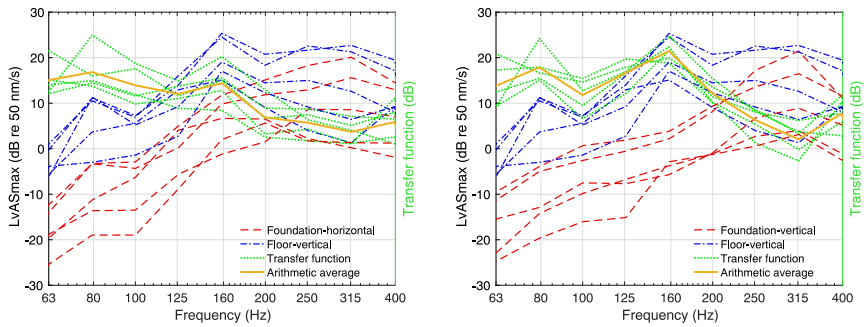

Figure 3.15: Vibration level and transfer function from foundation to floor at Prospect Hillgatan 10 in vertical and horizontal directions: (a) horizontal direction, (b) vertical direction.

Floor correction

The valid measurement conducted at Övre Fogelbergsgatan 1 was used to determine how vibration levels vary between different floors, as shown in Figure 3.16. The transfer function between different floors is calculated versus different frequencies. The mean value in the figures represents the arithmetic average attenuation per floor across all frequencies. According to the figures, regarding maximum level, floors 1 to 4 attenuate by 0.75 dB per floor, and floors 4 to 7 attenuate by 3.5 dB per floor, based on an arithmetic average over the valid frequency range. Therefore, vibration attenuates more on higher floors than on lower floors. Using only one value for all floors, the result is

-2 dB per floor, which is almost the same as other models ([19],[15]). Considering different frequencies, lower floors have greater attenuation than higher floors below 300 Hz. However, the situation is reversed for frequencies above 300 Hz.

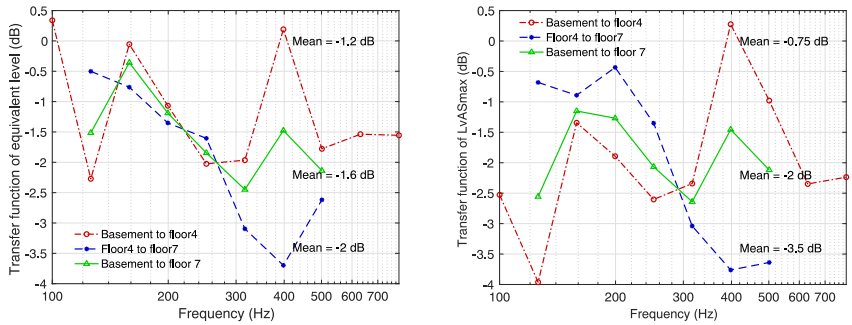

(a) (b)

Figure 3.16: Floor attenuation versus frequency and mean value of attenuation per each floor (Mean) in Övre Fogelbergsgatan 1, : (a) equivalent level, (b) maximum level (time-weighting Slow).

Vibration to noise correction

The data collected from Prospect Hillgatan 10 and Carlbergsgatan 13 were used to estimate the relationship between floor vibrations and ground-borne noise within the rooms. Figures 3.17 and 3.18 show transfer functions from floor vibration to sound pressure level in the corner of the room at Prospect Hillgatan 10 and Carlbergsgatan 13, respectively. According to Figures 3.17(a) and 3.18(a), the frequency range with a good signal-to-noise ratio, i.e., above 6 dB, is approximately between 60 and 400 Hz. Figures 3.17(b) and 3.18(b) show the maximum vibration level of the floor and the sound pressure level in the corner, as well as the transfer function between them for five freight trains at Prospect Hillgatan 10 and six freight trains at Carlbergsgatan 13 as a function of frequency. As can be seen from the figures, the average value of the transfer function is around 25 dB.

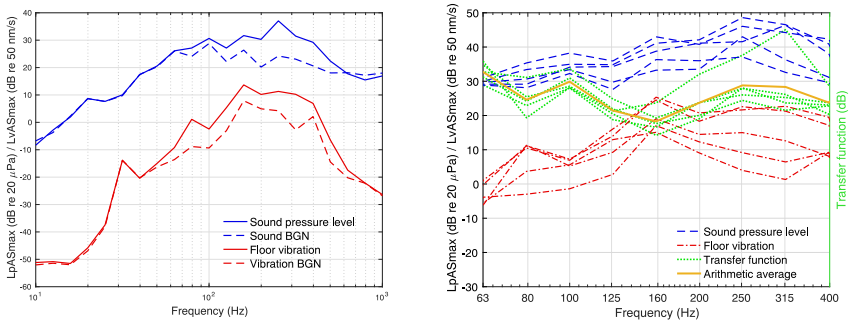

(a) (b)

Figure 3.17: Vibration level and transfer function from floor vibration to room ground-borne noise at prospect Hillgatan 10: (a) vibration and sound level, including background noise (BGN) for a single freight train, (b) transfer function for six freight trains.

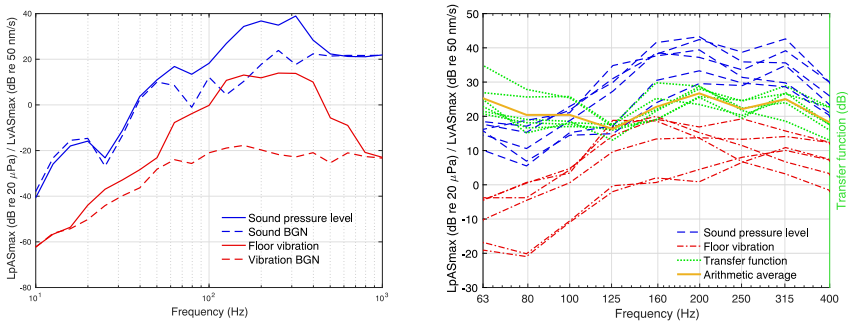

(a) (b)

Figure 3.18: Vibration level and transfer function from floor vibration to room ground-borne noise at Carlbergsgatan 13: (a) vibration and sound level, including background noise (BGN) for a single freight train, (b) transfer function for six freight trains.

In our measurements, the microphones were mounted in the corner of the rooms. There is a higher sound level near walls and in corner areas of rooms. The indicator of interest here is the average sound pressure level in the interior of the room. Figure 3.19 shows the transfer function from the sound pressure level in the corner of the room to the sound pressure level in the middle of the room in 1/3-octave bands. According to the figure, the transfer function varies between 1 to 10 dB at Prospect Hillgatan 10 and between -10 to 10 dB at Carlbergsgatan 13 at different frequencies.
Figure 3.20 shows the transfer function from floor vibration to sound pressure

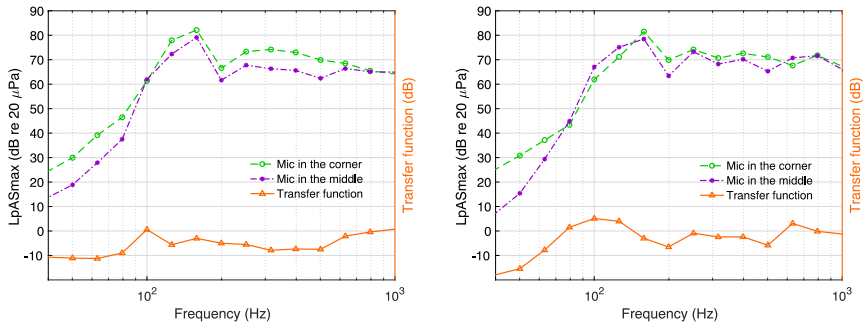

Figure 3.19: Transfer function from the microphone in the corner to the microphone in the middle: (a) Prospect Hillgatan 10, (b) Carlbergsgatan 13.

level in the middle of the room using the transfer function calculated from Figure 3.19.

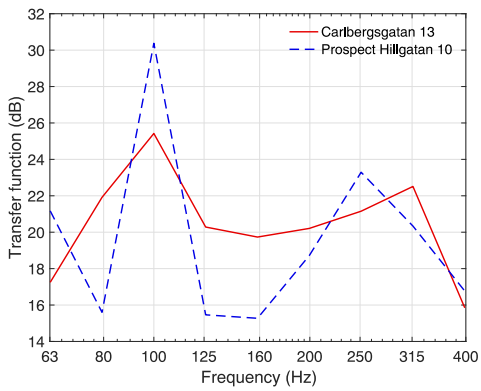

Figure 3.20: Transfer function from floor vibration to sound pressure level.

Room acoustic theory

The sound pressure level in a room can be estimated using Eq 3.3. It is employed to estimate the sound pressure level inside rooms at both Carlbergsgatan 13 and Prospect Hillgatan 10.

$$L_{\mathrm{p}} = L_{\mathrm{v}} + 10\log_{10}\sigma + 10\log_{10}\frac{4S}{A} \qquad \text{(dB)}. \tag{3.3}$$

The area of surfaces inside rooms (S) is 37.5 m^2 and the volume of rooms (V) is 15 m^3. The surfaces and volumes of both rooms are approximately the same. It is assumed that the whole surfaces inside the rooms vibrate and generate noises. It is also assumed that the radiation efficiency fulfills $\sigma = 1$ and T_{60} is considered to be 0.5 s. Replacing the parameters in Eq 3.3, the sound pressure level (L_{p})is as follows:

$$L_{\mathrm{p}} = L_{\mathrm{v}} + 14 \qquad (\mathrm{dB}). \tag{3.4}$$

According to Eq 3.4, the difference between vibration level and sound level inside the room is calculated as 14 dB. However, the results of measurements (Figure 3.20) show a difference of around 20 dB. One hypothesis is that the model of statistical room acoustics is not applicable in the small basement rooms which could partly account for the discrepancy. The Schroeder frequency for the rooms is around 370 Hz and this is clearly within the frequency range of interest (20–1000 Hz). This means uncertainty when using Eq 3.3 to calculate the sound pressure level inside these rooms.

3.3 Numerical results

Some results related to directivity, vibration on the ground surface, and vibration on the tunnel wall in the 2D simulation using the finite element method are explained here.

Figure 3.21 shows the radial directivity of vibration magnitude level for 2D calculations. The results are presented for six different 1/3-octave bands to show typical results at low frequencies (10 and 20 Hz), medium frequencies (80, 160 and 250 Hz) and high frequencies (1 kHz). According to the full space cases, vibration levels increase below the tunnel as the tunnel is present, and there is a tendency for vibration levels to decrease above the tunnel as it is added, but not for all directions, for example, right above. Below the tunnel, the full-space and half-space results are very similar, but above the tunnel, where the 2D evaluation positions reach the ground surface, where coupling between wave types occurs, and R-waves are present, they differ significantly. For the half-space and 1 kHz case, the directivity fluctuates violently depending on the direction and there is no clear reduction above the tunnel as the tunnel is added. However, above the tunnel, levels are generally lower than below the tunnel, indicating that most energy is transmitted downward.
Vibration levels in the y-direction are considered for the response at the ground surface. Typical results with and without tunnel from low to high frequencies are presented in Figure 3.22. The distance attenuation is clearly visible in the 1/3 octave band at 10 Hz. At high frequencies, interference effects between the wave types cause fluctuations. In the mid-frequency range, where S-wave

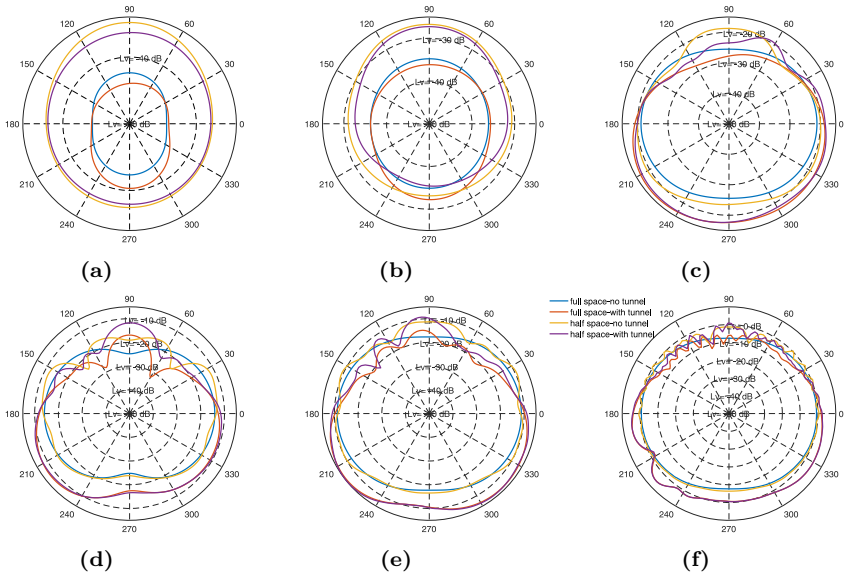

Figure 3.21: Directivity: (a) $f = 10$ Hz, (b) $f = 20$ Hz, (c) $f = 80$ Hz, (d) $f = 160$ Hz, (e) $f = 250$ Hz, (f) $f = 1$ kHz.

wavelength is on the order of tunnel width, the effect is stronger. These fluctuations increase when the wavelength of P-waves is smaller than the tunnel width. In general, the levels with the tunnel are significantly lower than without the tunnel, demonstrating that tunnel shielding reduces the velocities at the surface. The effect is smaller at low frequencies. At higher frequencies, the results start to fluctuate as a function of position and in general, the levels are approximately 4 to 10 dB lower for the shielded case. Additionally, the asymmetric directivity pattern due to the asymmetric position of the force is clear.

The results for receiver positions located along the tunnel floor and tunnel wall is shown in Figure 3.23. Tunnel floor vibrations are calculated in y-direction, while tunnel wall vibrations are calculated in both x- and y-directions. Figure 3.23(a) shows the vibration level in x and y-direction on the tunnel wall, and Figure 3.23(b) presents the same results normalized to the velocity in y-direction at the tunnel floor 1 m from the force. As expected, the velocity level is decreased on the tunnel floor by increasing the distance from the excitation point. The level in the y-direction at the tunnel wall decreases by increasing the height of the receiver position. In comparison, the velocity level in the x-direction is roughly the same, except at mid-frequency (about 50-200 Hz).

In general, the numerical results illustrate the importance of considering how the choice of reference position affects results. Our findings indicate a

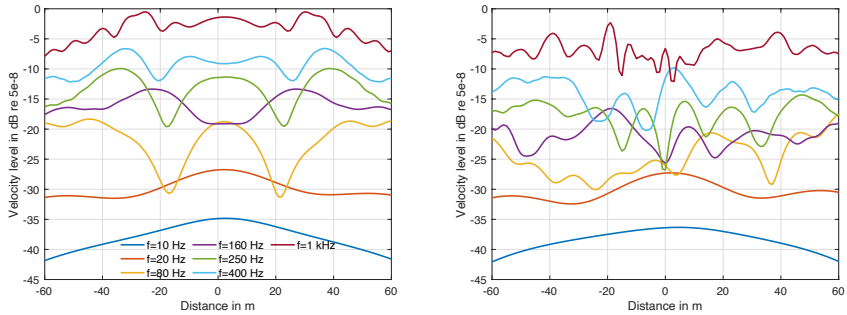

(a) (b)

Figure 3.22: Velocity level perpendicular to the ground surface: (a) half-space without the tunnel, (b) half-space with the tunnel. The legend shows the 1/3 octave center frequency in Hz.

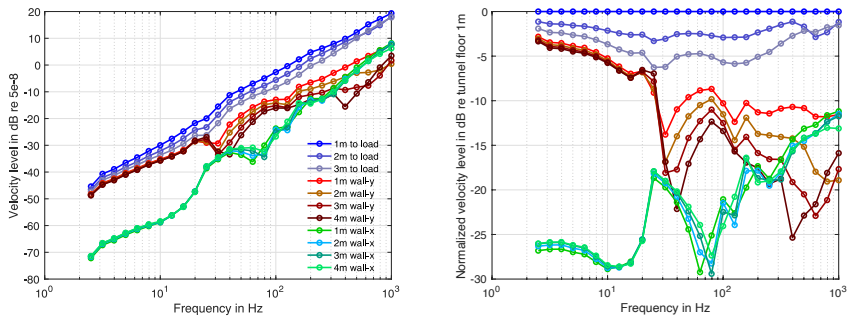

(a) (b)

Figure 3.23: Velocity level in 1/3 octave bands in the tunnel: (a) velocity level on the floor in the y-direction and on the tunnel wall in x and y-direction, (b) normalized velocity level on the floor in the y-direction and on the tunnel wall in x and y-direction.

significant reduction in vertical velocity, particularly at frequencies exceeding 20 Hz, as one moves from the tunnel floor to the tunnel wall. This reduction is even greater in the horizontal direction. The detailed information can be found in Part II.

CHAPTER 4

Summary of appended papers

Paper: Finite element modelling of tunnel shielding in vibration measurements of ground-borne noise

This paper aims to consider the tunnel shielding effect in terms of sensor position, sensor direction, and signal propagation up to 1 kHz using the finite element model. The tunnel shielding effect refers to how a tunnel cavity in bedrock with force excitation on the tunnel floor affects the vibration level on the tunnel wall and positions around the tunnel. An underground tunnel is modelled in 2D and 3D for a bedrock ground typical for Swedish conditions. It is found that the tunnel shielding effect decreases vibration levels above the tunnel and also causes significant fluctuations at higher frequencies (above 500 Hz).

Report: Ground Borne Noise Model and Methodology Description

The report develops a model and methodology suggested for ground-borne noise prediction in Swedish Transport Administration projects. The model has been adapted to Swedish bedrock conditions by measurements carried out in the Gårda tunnel in Gothenburg and by using existing data and results from measurements in the Åsa tunnel close to Varberg and the Håknäs tunnel along the Bothnia Line.

The methodology is formulated for three different stages based on precision and available information: location stage, planning stage, and construction stage. The first two stages correspond to planning and designing a railway track. The third stage involves the construction where more detailed information may be acquired. The prediction model presented here is developed

for Swedish bedrock from 20 Hz up to 1 kHz and formulated as a source term and several correction terms. These terms take into account various aspects, including train speed, distance attenuation, ground-to-building coupling, vibration levels on different floors and walls, how the room properties affect sound pressure levels within rooms, and different track treatments. Moreover, statistical approaches have been used to handle possible uncertainties in each term.

CHAPTER 5

Conclusions and Future Work

This work developed a methodology and a model for predicting ground-borne noise generated from railway tunnels for Swedish bedrock conditions. The model is developed using both numerical and empirical data sources. The empirical data were gathered from measurements carried out within the Gårda, Åsa, and Håknäs tunnels.

The modeling approach is based on three different stages, including the location stage, the planning stage, and the construction stage. In the location stage, the early phase of the project, the model predicts a single value. In the planning stage, the parameters are formulated as a function of frequency in 1/3-octave bands up to 1 kHz. The precision in the planning stage is greater than in the location stage. During the construction stage, site-specific measurements can be made using the tunnel under construction to verify the predictions made in the planning stage.

The prediction model (in Part III, Report) incorporates a source term and several correction terms, including train speed, distance attenuation, ground-to-building coupling, vibration levels on different floors, and the influence of room properties on sound pressure levels within rooms. Additionally, standard deviations related to each model term have been used to estimate uncertainty for the whole model.

Furthermore, in order to determine how vibration levels change with position in the tunnel, numerical analyses are conducted. The receiver positions are located along the tunnel floor and tunnel wall. As a result, from the tunnel floor to the tunnel wall, there is a clear reduction in vertical velocity above

20 Hz, and the horizontal velocity is even lower. This phenomenon can be called the tunnel shielding effect.

The model presented in this study focuses on railway tunnels and building foundations on bedrock. Further work can be done to extend its applicability to other cases, e.g., including ballast-free tracks and structural sound-dampening measures. To achieve this, additional measurement series are needed to ensure model accuracy and reliability in various contexts. There are various vibration sources such as hydraulic hammers that can be evaluated and used instead of trains to lower measurement costs. Special cases involving complex bedrock geometries or significant crack zones, which were not considered in the current model, offer potential areas for further development.

Furthermore, this model contains parameter values and formulas that may have to be refined as more experimental data become available in the future. By collecting continuous data and updating the model systematically, the model will be able to adapt to Swedish conditions over time.

There are uncertainties in different parts of the propagation path. These uncertainties include the source of vibration, vibration propagating from tunnels to structures, ground-to-building connections, and internal vibration propagation within the structure. These areas of potential influence need to be considered deeper in the further development of the model.

References

[1] Z. Xuetao, H. Jonasson, and K. Holmberg, "Source modelling of train noise-literature review and some initial measurements," 2000.

[2] Trafikverket, " Buller och vibrationer från trafik på väg och järnväg," TDOK 2014:1021, Dokumentdatum 2020-09-25, Version 3.0, Fastställt av Gäller från Ersätter Chef VO Planering 2021-01-01.

[3] R. Hood, R. Greer, M. Breslin, and P. Williams, "The calculation and assessment of ground-borne noise and perceptible vibration from trains in tunnels," *Journal of sound and vibration*, vol. 193, no. 1, pp. 215–225, 1996.

[4] Wikipedia, Seismic wave, `https://en.wikipedia.org/wiki/Seismic_wave`, 2023.

[5] L. Bergmann, H. Hatfield, *et al.*, "Ultrasonics and their scientific and technical applications," 1938.

[6] E. Ungar and E. Bender, "Vibrations produced in buildings by passage of subway trains; parameter estimation for preliminary design," Tech. Rep., 1975.

[7] R. D. Woods and L. P. Jedele, "Energy—attenuation relationships from construction vibrations," in *Vibration problems in geotechnical engineering*, ASCE, 1985, pp. 187–202.

[8] T. G. Gutowski and C. L. Dym, "Propagation of ground vibration: A review," *Journal of Sound and Vibration*, vol. 49, no. 2, pp. 179–193, 1976.

[9] E. Taniguchi and K. Sawada, "Attenuation with distance of traffic-induced vibrations," *Soils and foundations*, vol. 19, no. 2, pp. 15–28, 1979.

[10] A. Eitzenberger, "Wave propagation in rock and the influence of discontinuities," PhD thesis, Luleå University of Technology, 2012.

[11] L. J. Pyrak-Nolte, L. R. Myer, and N. G. Cook, "Anisotropy in seismic velocities and amplitudes from multiple parallel fractures," *Journal of Geophysical Research: Solid Earth*, vol. 95, no. B7, pp. 11 345–11 358, 1990.

[12] ISO, "Mechanical vibration – Ground-borne noise and vibration arising from rail systems – Part 1: General guidance," ISO 14837-1, 2005.

[13] B. Möller, R. Larsson, P.-E. Bengtsson, and L. Moritz, *Geodynamik i praktiken*, 2000.

[14] L. Hall, "Simulations and analyses of train-induced ground vibrations in finite element models," *Soil Dynamics and Earthquake Engineering*, vol. 23, no. 5, pp. 403–413, 2003.

[15] L. Kurzweil, "Ground-borne noise and vibration from underground rail systems," *Journal of Sound and Vibration*, vol. 66, no. 3, pp. 363–370, 1979.

[16] T. T. Commission *et al.*, *Yonge subway northern extension noise and vibration study*, 1976.

[17] H. J. Saurenman, R. L. Shipley, G. P. Wilson, I. Wilson, D. Cather, *et al.*, "In-service performance and costs of methods to control urban rail system noise," United States. Department of Transportation. Urban Mass Transportation ..., Tech. Rep., 1979.

[18] A. Eitzenberger, "Train-induced vibrations in tunnels: A review," 2008.

[19] D. A. T. Carl E. Hanson and L. D. Meister, *Transit noise and vibration impact assessment*. US Department of Transportation, Federal Transit Administration, 2006.

[20] L. Hannelius, "Earth vibration caused by heavy trains," *Jarnvagsteknik*, 1974.

[21] P. J. Remington, L. G. Kurzweil, and D. A. Towers, "Low-frequency noise and vibration from trains," *Transportation noise reference book*, 1987.

[22] J. Melke, "Noise and vibration from underground railway lines: Proposals for a prediction procedure," *Journal of Sound and Vibration*, vol. 120, no. 2, pp. 391–406, 1988.

[23] M. Villot, S. Bailhache, C. Guigou, and P. Jean, "Prediction of railway induced vibration and ground borne noise exposure in building and associated annoyance," in *Noise and Vibration Mitigation for Rail Transportation Systems*, Springer, 2015, pp. 289–296.

[24] M. Villot, P. Jean, L. Grau, and S. Bailhache, "Predicting railway-induced ground-borne noise from the vibration of radiating building elements using power-based building acoustics theory," *International Journal of Rail Transportation*, vol. 6, no. 1, pp. 38–54, 2018.

[25] G. Paneiro, F. Durão, M. C. e Silva, and P. F. Neves, "Prediction of ground vibration amplitudes due to urban railway traffic using quantitative and qualitative field data," *Transportation Research Part D: Transport and Environment*, vol. 40, pp. 1–13, 2015.

[26] J. Forrest and H. Hunt, "A three-dimensional tunnel model for calculation of train-induced ground vibration," *Journal of sound and vibration*, vol. 294, no. 4-5, pp. 678–705, 2006.

[27] X. Sheng, C. Jones, and D. Thompson, "Prediction of ground vibration from trains using the wavenumber finite and boundary element methods," *Journal of Sound and Vibration*, vol. 293, no. 3-5, pp. 575–586, 2006.

[28] P. Fiala, G. Degrande, and F. Augusztinovicz, "Numerical modelling of ground-borne noise and vibration in buildings due to surface rail traffic," *Journal of Sound and Vibration*, vol. 301, no. 3-5, pp. 718–738, 2007.

[29] K. Kuo, H. Verbraken, G. Degrande, and G. Lombaert, "Hybrid predictions of railway induced ground vibration using a combination of experimental measurements and numerical modelling," *Journal of Sound and Vibration*, vol. 373, pp. 263–284, 2016.

[30] R. Arcos, P. J. Soares, P. A. Costa, and L. Godinho, "An experimental/numerical hybrid methodology for the prediction of railway-induced ground-borne vibration on buildings to be constructed close to existing railway infrastructures: Numerical validation and parametric study," *Soil Dynamics and Earthquake Engineering*, vol. 150, p. 106 888, 2021.

[31] J. Manning, R. Cann, J. Fredberg, *et al.*, "Prediction and control of rail transit noise and vibration-a state-of-the-art assessment," United States. Urban Mass Transportation Administration, Tech. Rep., 1974.

[32] G. Wilson, "Ground-borne vibration levels from rock and earth base subways," *Report. Wilson Ihrig & Associates Inc., Oakland, California, US*, 1971.

[33] RENVIB II Final Report Phase 1 and Phase 2; ERRI Utrecht, 2000.

[34] V. Jurdic, O. Bewes, R. Greer, and T. Marshall, "Developing prediction model for ground-borne noise and vibration from high speed trains running at speeds in excess of 300km/h," in *The 21st International Congress on Sound and Vibration (ICSV)*, Beijing/China, 2014.

[35] R. Greer, "Methods for predicting groundborne noise and vibration from trains in tunnels," in *Local Authority Railway Impact Forum (LARIF)*, 1999.

[36] J. T. Nelson, H. J. Saurenman, I. Wilson, *et al.*, "State-of-the-art review: Prediction and control of groundborne noise and vibration from rail transit trains," 1983.

[37] Trafikverket, " Banunderbyggnad i tunnlar för ballastspår och ballastfria spårkonstruktioner," Document, Trafikverket, 2020.

[38] M. Källman, "Mätrapport - Långtidsmätning av vibrationer i Åsatunneln," ÅF Infrastructure AB, Tech. Rep., 2020.

[39] T. Odebrant, "Höghastighetsprojektet. Stomljud. Slutrapport," PM10. Uppdragsnummer 552777. Trafikverket, Tech. Rep., 2010.

[40] I. BIPM, I. Ifcc, I. Iso, and O. Iupap, "Evaluation of measurement data—guide to the expression of uncertainty in measurement, jcgm 100: 2008 gum 1995 with minor corrections," *Joint Committee for Guides in Metrology*, 2008.